ELSEVIER

Brain & Development 34 (2012) 861–865

BRAIN & DEVELOPMENT
Official Journal of the Japanese Society of Child Neurology

www.elsevier.com/locate/braindev

Case report

Two Japanese patients with Leigh syndrome caused by novel *SURF1* mutations

Junpei Tanigawa [a], Kaori Kaneko [c], Masakazu Honda [d], Hiroko Harashima [d], Kei Murayama [e], Takahito Wada [a], Kyoko Takano [a], Mizue Iai [a], Sumimasa Yamashita [a], Hiroko Shimbo [a], Noriko Aida [b], Akira Ohtake [d], Hitoshi Osaka [a,*]

[a] *Division of Neurology, Kanagawa Children's Medical Center, Yokohama 232-8555, Japan*
[b] *Division of Radiology, Kanagawa Children's Medical Center, Yokohama 232-8555, Japan*
[c] *Division of Pediatric Neurology, Yokohama Ryoiku-iryo Center, Yokohama 241-0014, Japan*
[d] *Department of Pediatrics, Faculty of Medicine, Saitama Medical University, Saitama 350-1241, Japan*
[e] *Department of Metabolism, Chiba Children's Hospital, Chiba 266-0007, Japan*

Received 7 November 2011; received in revised form 11 February 2012; accepted 13 February 2012

Abstract

We report two patients with Leigh syndrome that showed a combination of facial dysmorphism and MRI imaging indicating an *SURF1* deficiency, which was confirmed by sequence analysis. Case 1 is a 3-year-old girl with failure to thrive and developmental delay. She presented with tachypnea at rest and displayed facial dysmorphism including frontal bossing, lateral displacement of inner canthi, esotropia, maxillary hypoplasia, slightly upturned nostril, and hypertrichosis dominant on the forehead and extremities. Case 2 is an 8-year-old boy with respiratory failure. He had been diagnosed as selective complex IV deficiency. Case 2 displayed facial dysmorphism and hypertrichosis. Since both patients displayed characteristic facial dysmorphism and MRI findings, we sequenced the *SURF1* gene and identified two heterozygous mutations; c.49+1 G>T and c.752_753del in Case 1, and homozygous c.743 C>A in Case 2. For patients with Leigh syndrome showing these facial dysmorphism and hypertrichosis, sequence analysis of the *SURF1* gene may be useful.

Keywords: Leigh syndrome; *SURF1* deficiency; Facial dysmorphism; Hypertrichosis

1. Introduction

Leigh syndrome (OMIM 256000) is a progressive neurodegenerative disorder with the usual onset in infancy or early childhood. It is a genetically heterogeneous disease and the most common cause is a molecular defect in mitochondrial energy production system, including the respiratory chain complexes and pyruvate dehydrogenase complex. An isolated generalized defect of complex IV, (Cytochrome C oxidase) is the most common biochemical abnormalities found in Leigh syndrome [1]. Leigh syndrome with *SURF1* mutations, which encode the putative assembly protein of complex IV, have been reported [2] with specific clinical features of facial dysmorphism [3], hypertrichosis [4], and MRI findings [5]. Here, we report two patients with these clinical features and novel *SURF1* mutations.

* Corresponding author. Address: Division of Neurology, Kanagawa Children's Medical Center, 2-138-4 Mutsukawa, Minami-ku, Yokohama 232-8555, Japan. Tel.: +81 45 711 2351; fax: +81 45 721 3324.
E-mail address: hosaka@kcmc.jp (H. Osaka).

0387-7604/$ - see front matter © 2012 The Japanese Society of Child Neurology. Published by Elsevier B.V. All rights reserved.
doi:10.1016/j.braindev.2012.02.007

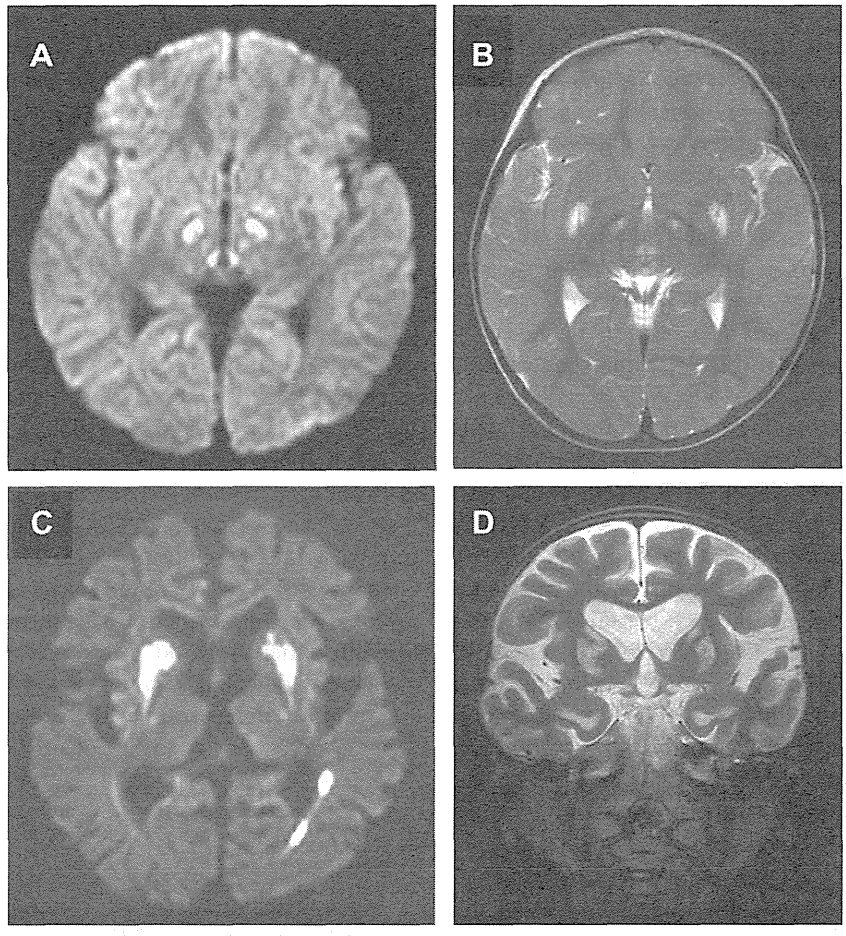

Fig. 1. Diffusion-weighted (A and C) and T2-weighted (B and D) magnetic resonance imaging of the brain in Case 1 at 2 years and 5 months of age (A and B), and in Case 2 at 7 years and 6 months of age (C and D). In Case 1, the bilateral substantia nigra (A), subthalamic nucleus (A and B), red nucleus (A), medial parts of the midbrain (A and B) and putamen (B) show the signal hyperintensity. In Case 2, bilateral striatum reveal hypeintensity (C and D). The left optic radiation is also involved in Case 2 (C) and the global cerebral hemisphere is atrophic (C and D).

2. Case reports

2.1. Case 1

Case 1 is 3-year-old female that was referred to our hospital for an evaluation of failure to thrive and developmental delay at 2 years. She was born to healthy nonconsanguineous Japanese parents. The neonatal period was unremarkable. She held her head upright at 3 months of age, and sat at the 6 months. At the 9 months, she was able to walk independently while holding on to furniture. Her development did not progress thereafter, and she has not walked alone and only speaks using jargon. She was conscious, alert and presented with tachypnea at rest. She displayed facial dysmorphism including frontal bossing, lateral displacement of inner canthi, esotropia, maxillary hypoplasia, slightly upturned nostril, and hypertrichosis dominant on the forehead and extremities. Mild opthalmoplegia and ptosis were noted. She manifested generalized mild hypotonia, truncal ataxia and normal deep tendon reflexes with negative Babinski's signs. Serum lactate was elevated at 35.7 mg/dl. MRI showed signal hyperintensity of the bilateral putamen, subthalamic nucleus, red nucleus and brain stem on T2-weighted images (T2WI) and diffusion-weighted images (DWI) (Fig. 1). The enzyme analysis of the respiratory chain complexes were not performed in this patient.

2.2. Case 2

Case 2 is 8-year-old male on ventilation that was transferred to our hospital for tracheostomy. He was born at term to healthy, nonconsanguineous parents. He had been able to get cruising by 12 months. At 19 months, he presented with neurodevelopmental regression and ataxia. Laboratory investigation revealed elevated cerebrospinal fluid lactate and pyruvate. Brain MRI showed signal hyperintensity of the bilateral basal ganglia, midbrain and medulla oblongata on T2WI. Fibroblast analysis confirmed a decreased amount and activity of complex IV in the respiratory chain complexes

(Fig. 2). He displayed facial dysmorphism including synophrys and micrognathia, hypertrichosis, thoracic deformity and generalized hypotonia and elevated deep tendon reflexes with positive Babinski's signs. MRI showed that the bilateral cerebral hemisphere were globally atrophic and signal hyperintensity of the bilateral optic radiation, putamen, basal ganglia including subthalamic nucleus, and brain stem on T2WI. The left optic radiation, bilateral putamen and globus pallidus also showed high signal intensity on DWI (Fig. 1).

3. Genomic DNA sequencing, RT-PCR and sequencing

Genomic DNA was prepared from white blood cells using the Wizard Genomic DNA purification kit (Promega, Madison, WI, USA). PCR of all exons and exon–intron boundaries of the *SURF1* gene was performed with specific primers using Ex Taq PCR version 1.0 kit (Takara, Shiga, Japan) according to the manufactures instruction (Suppl. Table 1). Total RNA was extracted from leukocytes using Trizol reagent and amplified with the SMART™ mRNA amplification method (Clontech, Mountain View, CA). The amplified mRNA was subjected to reverse transcription with Prime Script reverse transcriptase (Takara, Shiga, Japan) using Oligo (dT) primers. RT-PCR was performed using primers at exons 1 and 9 of the *SURF1* gene, according to the manufacture's instruction (Suppl. Table 1). Patients and families participating in the gene analysis gave written informed consent to the gene analysis, which was approved by the ethical committee of Kanagawa Children's Medical Center.

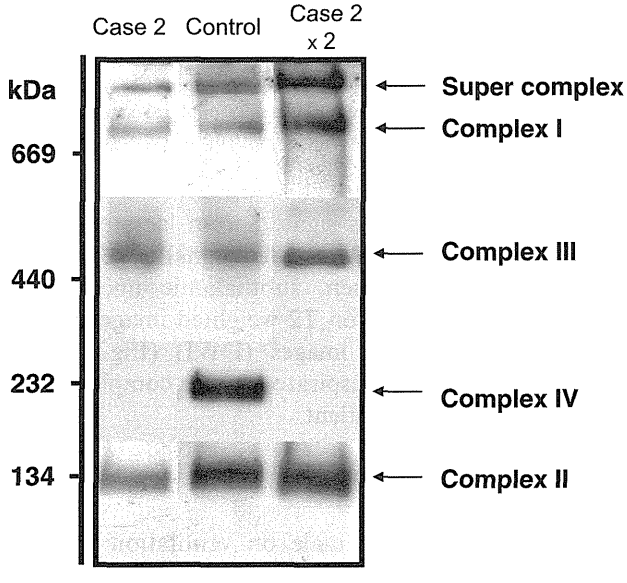

Fig. 2. Analysis of respiratory chain complex amount by blue native polyacrylamide gel electrophoresis in Case 2. Mitochondria isolated from Case 2 and normal control fibroblasts were solubilized in dodecyl maltoside and subjected to BN-PAGE and Western blotting [9]. In x 2 lane, the amount of protein loaded was twice. The amount of fully assembled complex IV was shown to be dramatically decreased in Case 2. The amount of complexes I, II, and III were all comparable to those in the normal control. In vitro enzyme assay [10] also revealed deficiencies of complex IV: the activities of complex I, II, III and IV relative to that of citrate synthase were 137%, 238%, 124% and 12%, respectively.

4. Results

4.1. Case 1

We identified two novel heterozygous mutations: a maternal c.49+1 G>T splice site mutation in intron 1 and a paternal c.752_753del in exon 8. This deletion resulted in a frame shift at amino acid 251(Gln251) causing a stop codon in exon 8 (Fig. 3). The c.49+1 G>T splice site mutation changes the highly conserved G nucleotide at position +1 of the donor splice site (5′ss) in intron 1. We attempted to characterize the splicing outcome of this sequence variation by RT-PCR analysis from patient's blood. Sequence analysis of the RT-PCR reaction detected only the allele with the c.752_753delAG mutation, which implies the presence of a nonsense mediated decay or instability of mRNA from the allele with the c.49+1 G>T splice site mutation.

4.2. Case 2

Sequence analysis of the *SURF1* gene revealed a novel homozygous c.743 C>A, p.Ala248Asp in exon 7. Both parents of this patient were heterozygous for this mutation (Fig. 3). This mutation changes highly conserved Alanine to Aspartate. This mutation was not found in 100 control alleles.

5. Discussion

Molecular elucidation of Leigh syndrome is challenging since many enzymes are involved, such as mitochondrial respiratory chain complexes I, II, III, IV, and V, and components of the pyruvate dehydrogenase complex. Mutation analysis in DNA is more complicated, even after focusing on respiratory complex IV. Mitochondrial-encoded *MTCO3* and nuclear-encoded *COX10*, *COX15*, *SCO2*, and *SURF1*, have been reported as the cause of Leigh syndrome [6,7]. Our two cases presented with mental retardation, failure to thrive, respiratory dysfunction, facial dysmorphism and hypertrichosis. Facial dysmorphism including micrognathia and hypertrichosis especially in the extremities have been reported to be distinctive and characteristic feature of *SURF1* gene mutation [3,4]. Our two cases underscore the importance of *SURF1* analysis in Leigh syndrome with facial dysmorphism and hypertrichosis. However, not all patients with this gene mutation carry these symptoms. Although facial dysmorphism has been also

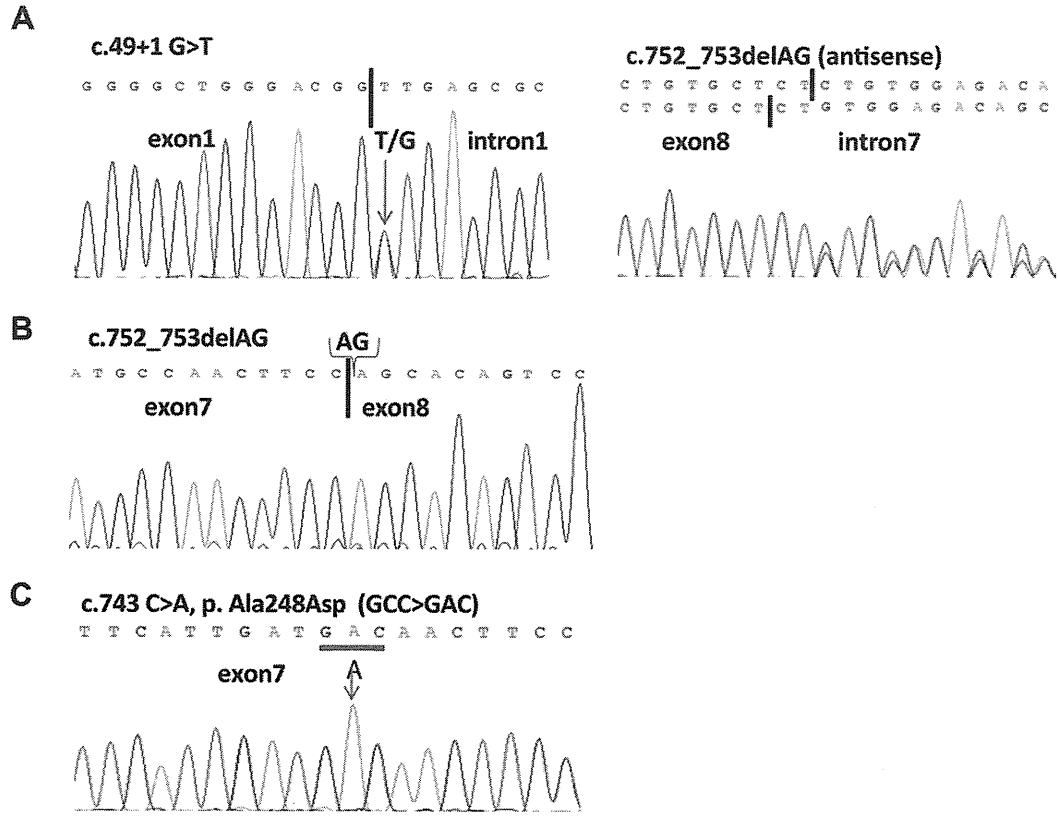

Fig. 3. Analysis of the *SURF1* gene. A chromatogram of the two novel heterozygous mutations; c.49+1 G>T and c.752_753del in Case 1 (A) and homozygous c.743 C>A in Case 2 (C). Panel B shows the chromatogram of cDNA from Case 1. The mutations are shown on the sense strand except for the right panel of A (antisense).

reported in Leigh syndrome with pyruvate dehydrogenase complex, hypertrichosis has not been described [8].

To date, more than 100 patients of Leigh disease with *SURF1* mutations have been reported [6,7]. To our knowledge, this is the first report of a mutation in intron 1, suggesting the need to scan whole exons and exon/intron boundaries.

Common MRI findings of Leigh syndrome are symmetric lesions in the brainstem, basal ganglia, thalamus and spinal cord, Leigh syndrome with *SURF1* mutation have been reported to involved the subthalamic nuclei, medulla, inferior cerebellar peduncles, and substantia nigra [5]. In addition, Case 2 showed signal hyperintensities in bilateral optic radiation on T2WI and DWI, which has not been reported previously in Leigh syndrome with *SURF1* mutations. Since Case 2 had never shown severe hypoxemia, this finding may be significant in patients with *SURF1* mutation or may appear in a progressed stage of disease.

Acknowledgements

This work was supported in part by Grants-in-Aid from Scientific Research from the Ministry of Health, Labor and Welfare of Japan, Health and Labor Science Research Grant of Japan, Yokohama Foundation for Advancement of Medical Science, Takeda Science Foundation, Kanagawa Municipal Hospital Pediatric Research and a grant of the Innovative Cell Biology by Innovative Technology (Cell Innovation Program) from the Ministry of Education, Culture, Sports, Science and Technology, Japan.

Appendix A. Supplementary data

Supplementary data associated with this article can be found, in the online version, at doi:10.1016/j.braindev.2012.02.007.

References

[1] Rahman S, Blok RB, Dahl HH, Danks DM, Kirby DM, Chow CW, et al. Leigh syndrome: clinical features and biochemical and DNA abnormalities. Ann Neurol 1996;39:343–51.
[2] Zhu Z, Yao J, Johns T, Fu K, De Bie I, Macmillan C, et al. SURF1, encoding a factor involved in the biogenesis of cytochrome c oxidase, is mutated in Leigh syndrome. Nat Genet 1998;20:337–43.
[3] Yüksel A, Seven M, Cetincelik U, Yeşil G, Köksal V. Facial dysmorphism in Leigh syndrome with SURF-1 mutation and COX deficiency. Pediatr Neurol 2006;34:486–9.
[4] Ostergaard E, Bradinova I, Ravn SH, Hansen FJ, Simeonov E, Christensen E, et al. Hypertrichosis in patients with SURF1 mutations. Am J Med Genet A 2005;138:384–8.

[5] Rossi A, Biancheri R, Bruno C, Di Rocco M, Calvi A, Pessagno A, et al. Leigh Syndrome with COX deficiency and SURF1 gene mutations: MR imaging findings. AJNR Am J Neuroradiol 2003;24:1188–91.
[6] Shoubridge EA. Cytochrome c oxidase deficiency. Am J Med Genet 2001;106:46–52.
[7] Böhm M, Pronicka E, Karczmarewicz E, Pronicki M, Piekutowska-Abramczuk D, Sykut-Cegielska J, et al. Retrospective, multicentric study of 180 children with cytochrome C oxidase deficiency. Pediatr Res 2006;59:21–6.
[8] Robinson BH, MacMillan H, Petrova-Benedict R, Sherwood WG. Variable clinical presentation in patients with defective E1 component of pyruvate dehydrogenase complex. J Pediatr 1987;111:525–33.
[9] Kirby DM, Salemi R, Sugiana C, Ohtake A, Parry L, Bell KM, et al. NDUFS6 mutations are a novel cause of lethal neonatal mitochondrial complex I deficiency. J Clin Invest 2004;114: v837–845.
[10] Murayama K, Nagasaka H, Tsuruoka T, Omata Y, Horie H, Tregoning S, et al. Intractable secretory diarrhea in a Japanese boy with mitochondrial respiratory chain complex I deficiency. Eur J Pediatr 2009;168:297–302.

Molecular Genetics and Metabolism 106 (2012) 474–477

Contents lists available at SciVerse ScienceDirect

Molecular Genetics and Metabolism

journal homepage: www.elsevier.com/locate/ymgme

Metabolic autopsy with postmortem cultured fibroblasts in sudden unexpected death in infancy: Diagnosis of mitochondrial respiratory chain disorders

Takuma Yamamoto [a,*,1], Yuko Emoto [a,1], Kei Murayama [b], Hidekazu Tanaka [c], Yukiko Kuriu [a], Akira Ohtake [d], Ryoji Matoba [a]

[a] Department of Legal Medicine, Osaka University Graduate School of Medicine, 2-2 Yamada-Oka, Suita, Osaka 565-0871, Japan
[b] Department of Metabolism, Chiba Children's Hospital, 579-1, Henda-cho, Midori-ku, Chiba 266-0007, Japan
[c] Department of Pharmacology, Osaka University Graduate School of Medicine, 2-2 Yamada-Oka, Suita, Osaka 565-0871, Japan
[d] Department of Pediatrics, Saitama Medical University, 38, Morohongoh, Moroyama, Saitama 350-0495, Japan

ARTICLE INFO

Article history:
Received 7 May 2012
Accepted 7 May 2012
Available online 11 May 2012

Keywords:
Metabolic autopsy
Postmortem cultured fibroblasts
Mitochondrial respiratory chain disorders
Sudden unexpected death in infancy

ABSTRACT

Mitochondrial respiratory chain disorders are the most common disorders among inherited metabolic disorders. However, there are few published reports regarding the relationship between mitochondrial respiratory chain disorders and sudden unexpected death in infancy. In the present study, we performed metabolic autopsy in 13 Japanese cases of sudden unexpected death in infancy. We performed fat staining of liver and postmortem acylcarnitine analysis. In addition, we analyzed mitochondrial respiratory chain enzyme activity in frozen organs as well as in postmortem cultured fibroblasts. In heart, 11 cases of complex I activity met the major criteria and one case of complex I activity met the minor criteria. In liver, three cases of complex I activity met the major criteria and four cases of complex I activity met the minor criteria. However, these specimens are susceptible to postmortem changes and, therefore, correct enzyme analysis is hard to be performed. In cultured fibroblasts, only one case of complex I activity met the major criteria and one case of complex I activity met the minor criteria. Cultured fibroblasts are not affected by postmortem changes and, therefore, reflect premortem information more accurately. These cases might not have been identified without postmortem cultured fibroblasts. In conclusion, we detected one probable case and one possible case of mitochondrial respiratory chain disorders among 13 Japanese cases of sudden unexpected death in infancy. Mitochondrial respiratory chain disorders are one of the important inherited metabolic disorders causing sudden unexpected death in infancy. We advocate metabolic autopsy with postmortem cultured fibroblasts in sudden unexpected death in infancy cases.

1. Introduction

Sudden unexpected death in infancy (SUDI) is defined as sudden unexpected death occurring before 12 months of age. If SUDI remains unexplained after thorough investigations, it is classified as sudden infant death syndrome (SIDS). The more common causes of SUDI are infection, cardiovascular anomaly, child abuse, and metabolic disorders. However, the many potential inherited metabolic disorders are more difficult to diagnose at autopsy as compared to cardiovascular defects and serious infection. Inherited metabolic disorders may, therefore, be underdiagnosed as a cause of SUDI or misdiagnosed as SIDS. Fatty acid oxidation disorders (FAODs) are one type of the inherited metabolic disorders and may cause as much as 5% of SUDI cases after thorough investigations including metabolic autopsy [1–5]. In a review of SUDI cases with respect to potential FAODs, we found a case of carnitine palmitoyltransferase II deficiency [6]. In that study, we performed fat staining of liver, postmortem acylcarnitine analysis, and genetic analysis, advocating the importance of metabolic autopsy in SUDI cases.

Mitochondrial respiratory chain (MRC) disorders were first identified in 1962 [7]. MRC disorders have a frequency of about at least 1:5000 newborns and are the most common disorders among inherited metabolic disorders [8]. However, there are few published reports regarding the relationship between MRC disorders and SUDI. Studies of MRC disorders have not progressed because of technical difficulties or variability in clinical manifestations [9]. In sudden death cases especially, clinical features are unclear and postmortem changes complicate molecular analysis.

In the present study, we performed metabolic autopsy in 13 Japanese cases of SUDI in order to determine whether MRC disorders could be detected or not. We performed fat staining of liver and postmortem

Abbreviations: CS, citrate synthetase; FAODs, fatty acid oxidation disorders; MRC, mitochondrial respiratory chain; OXPHOS, oxidative phosphorylation; SIDS, sudden infant death syndrome; SUDI, sudden unexpected death in infancy.

* Corresponding author. Fax: +81 6 6879 3119.
E-mail address: yamamoto@legal.med.osaka-u.ac.jp (T. Yamamoto).

[1] These authors contributed equally to this work.

1096-7192/$ – see front matter © 2012 Elsevier Inc. All rights reserved.
doi:10.1016/j.ymgme.2012.05.002

acylcarnitine analysis according to the previous methods. In addition, we analyzed MRC enzyme activity in frozen organs as well as in postmortem cultured fibroblasts. With such metabolic autopsy, we were able to detect one probable case and one possible case of MRC disorders. These cases might not have been identified without metabolic autopsy. MRC disorders are important diseases causing SUDI and metabolic autopsy might be helpful for forensic scientists and pediatricians to diagnose MRC disorders that might not otherwise be identified.

2. Materials and methods

2.1. Subjects

Between October 2009 and September 2011, forensic autopsy was performed on 588 cases at our institute, 22 of whom were under 12 months of age. Following macroscopic examination, nine cases could be diagnosed but 13 cases (Table 1) did not have any characteristic appearance and remained undiagnosed. In this study, we reviewed these 13 undiagnosed cases (8 males, 5 females) with age ranging from 1 to 10 months.

2.2. Autopsy

Autopsies were performed within 24 h following death. Blood was obtained from the femoral vein. Heart and liver specimens were immediately cut and frozen at −80 °C. Dermis, which was cut and sterilized, was cultured at 37 °C and 5% CO_2 in Dulbecco's modified Eagle's medium (Sigma, St. Louis, MO) containing 10% fetal bovine serum, 1% penicillin streptomycin glutamine, and 2.5% amphotericin B (Life Technologies, Indianapolis, IN). Once cultures were established, fibroblasts were frozen at −80 °C.

2.3. Sudan III staining

Liver samples preserved in 4% phosphate-buffered formaldehyde solution were frozen, cut into 10-μm sections, and stained by the Sudan III method for fat staining.

2.4. Postmortem blood acylcarnitine analysis by tandem mass spectrometry

Whole blood samples obtained at autopsy were blotted onto one spot on Guthrie cards. They were subjected to acylcarnitine analysis by tandem mass spectrometry and compared with the previously determined normal range [6].

Table 1
SUDI cases.

Case no.	Age/sex	Height/weight (cm/kg)	Circumstances	Fever	Remarks
1	4 mo/M	68/7.5	Sleeping	−	
2	10 mo/F	70/8.8	Sleeping	−	Sister: undiagnosed encephalitis
3	10 mo/F	71/7.7	Sleeping	+	Cesarean section
4	9 mo/M	67/7.5	Sleeping	−	
5	4 mo/M	60/5.7	Sleeping	−	Hydrocephalia
6	6 mo/M	68/8.0	Sleeping	−	
7	1 mo/F	51/3.6	Sleeping	−	Twins, preterm birth
8	10 mo/M	72/9.9	Sleeping	−	Developmental disease (right side of the body paralysis)
9	6 mo/F	64/8.9	Sleeping	−	Bronchitis
10	4 mo/M	65/7.4	Sleeping	−	Cesarean section
11	1 mo/M	58/4.8	Sleeping	−	
12	5 mo/M	59/4.2	Sleeping	−	Preterm birth
13	2 mo/F	53/3.9	Sleeping	−	Low-birth-weight infant

Abbreviations: F, female; M, male; mo, month; SUDI, sudden unexpected death in infancy.

2.5. Enzyme analysis

The activity of mitochondrial respiratory chain complexes I, II, III, and IV was assayed in the crude post-600-g supernatant of heart and liver, and in isolated mitochondria from skin fibroblasts as described previously [10]. The activity of each complex was presented as a percent ratio relative to the mean value [9]. The activity of complexes I, II, III, and IV was also calculated as the percent relative to citrate synthetase (CS), a mitochondrial enzyme marker or complex II activity [10].

2.6. Ethics

This study was approved by the Ethics Committee of the Osaka University Graduate School of Medicine.

3. Results

3.1. Microscopic examination

One of the common features in diagnosing MRC disorders is hepatic steatosis. We therefore performed Sudan III staining to examine whether vacuoles caused by fatty degeneration were present in hepatocytes. Diffuse microvesicular steatosis was detected in case 5 (Fig. 1A). No Sudan III-positive vacuole was detected in case 13 (Fig. 1B) and the other cases, for example, case 2 (Fig. 1C).

3.2. Postmortem blood acylcarnitine analysis

We performed acylcarnitine analysis by tandem mass spectrometry using whole blood samples. In all samples, data were within the normal range. These data suggested that no case was affected by FAODs (data not shown).

3.3. Enzyme analysis of MRC complexes in heart, liver, and cultured fibroblasts

The enzyme activity of each complex was compared with the CS ratio and complex II ratio. Lower than 20% activity of any complex in a tissue or lower than 30% activity of any complex in a cell line meets the major criteria. Lower than 30% activity of any complex in a tissue or lower than 40% activity of any complex in a cell line meets the minor criteria according to Bernier et al. [11].

In heart, 11 cases of complex I activity met the major criteria of MRC disorders and one case of complex I activity met the minor criteria (Fig. 2A). In liver, three cases of complex I activity met the major criteria of MRC disorders and four cases of complex I activity met the minor criteria (Fig. 2B). In cultured fibroblasts, one case (case 5) of complex I activity met the major criteria of MRC disorders and one case (case 13) of complex I activity met the minor criteria (Fig. 2C, Table 2). The activity of complexes II, III, and IV was maintained in almost all cases.

3.4. Diagnosis

A definite diagnosis is defined as the identification of either two major criteria or one major plus two minor criteria. A probable diagnosis is defined as either one major plus one minor criterion or at least three minor criteria. A possible diagnosis is defined as either a single major criterion or two minor criteria, one of which must be clinical [11].

All the cases had a clinical symptom of sudden death, meeting one minor criterion. In the enzyme activity, eleven cases (cases 2, 4–13) met the major criteria and we could make a probable diagnosis in these 11 cases. The other two cases (cases 1 and 3) met the minor criteria and we could make a possible diagnosis.

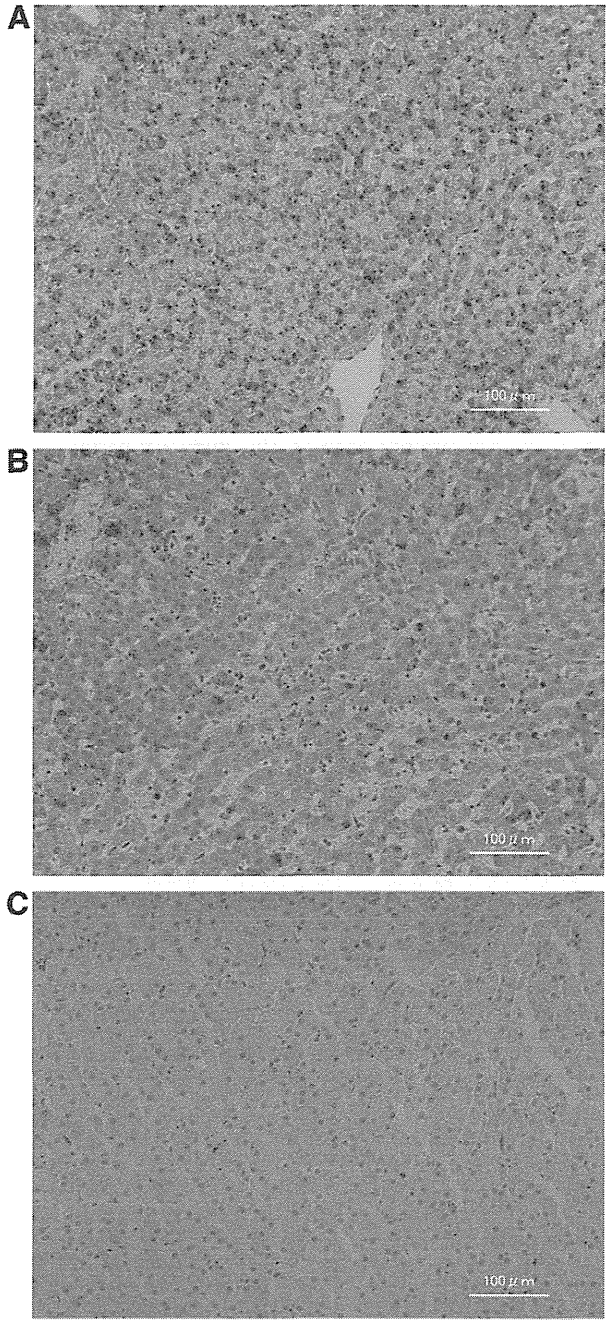

Fig. 1. Microscopic examination of liver (Sudan III staining): (A) case 5, (B) case 13, and (C) case 2. Diffuse microvesicular steatosis was detected in case 5 (A). No Sudan III-positive vacuole was detected in case 13 (B) and the other cases, for example, case 2 (C).

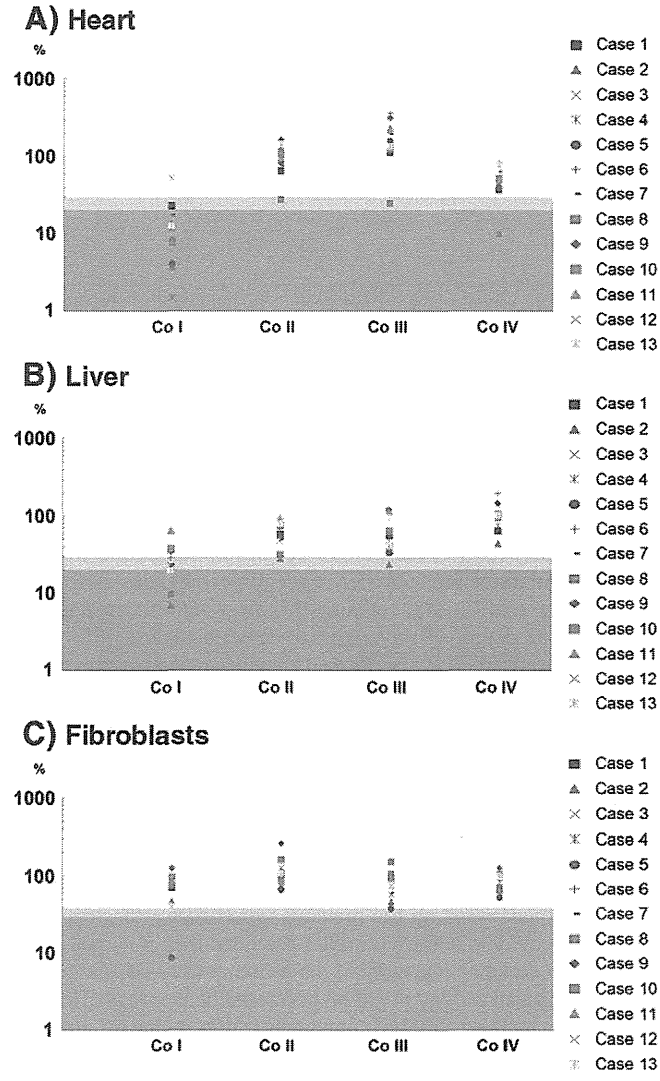

Fig. 2. Enzyme activity of MRC complexes in heart (A), liver (B), and cultured fibroblasts (C). In heart, 11 cases of complex I activity were under 20% of the CS ratio, meeting the major criteria and one case of complex I activity was under 30% of the CS ratio, meeting the minor criteria (A). In liver, three cases of complex I activity were under 20% of the CS ratio, meeting the major criteria and four cases of complex I activity were under 30% of the CS ratio, meeting the minor criteria (B). In cultured fibroblasts, one case (case 5) of complex I activity was under 30% of the CS ratio, meeting the major criteria and one case (case 13) of complex I activity was under 40% of the CS ratio, meeting the minor criteria (C). The activity of complexes II, III, and IV was maintained in almost all cases. The enzyme activity of each complex was compared with the CS ratio. Lower than 20% activity in a tissue or lower than 30% activity in a cell line (dark blue) meets the major criteria. Lower than 30% activity in a tissue or lower than 40% activity in a cell line (light blue) meets the minor criteria.

4. Discussion

Mitochondria are essential organelles that exist in all nucleated mammalian cells. They provide the energy required for normal cell function through oxidative phosphorylation (OXPHOS). OXPHOS includes MRC complexes (complexes I, II, III, and IV) and ATP synthase (complex V) [12], which use reduced coenzymes from the tricarboxylic acid cycle and molecular oxygen, generating cellular energy in the form of ATP [13].

The infantile or early neonatal period demands high energy. Patients with MRC disorders are unable to produce adequate energy, which may thus compromise them in the first days of life or during infancy. MRC disorders affect most organ systems and present variable clinical manifestations from prenatal complications through acute neonatal decompensation and death to adult-onset disorders. Therefore, it is not surprising that MRC disorders are also one of the causes of SUDI. However, there are few reports on a relationship between MRC disorders and SUDI [12,14].

We have previously reviewed SUDI cases with respect to FAODs and found a case of carnitine palmitoyltransferase II deficiency [6]. In that study, we advocated the importance of metabolic autopsy [15], including fat staining of liver, postmortem acylcarnitine analysis, and genetic analysis. Using this protocol, most FAODs, some amino acid oxidation disorders, and some organic acid oxidation disorders could be diagnosed.

However, MRC disorders are difficult to diagnose. First, they present variable clinical manifestations and non-specific features such as failure to thrive or hepatic, cardiac, renal, gastrointestinal, endocrine, hematological, or other symptoms [10,16]. Second, although blood

Table 2
Enzyme assay of mitochondrial respiratory chain complexes in cultured fibroblasts.

	Enzyme activity (%)[a]			
	Co I	Co II	Co III	Co IV
Case 5				
CS ratio	9	66	38	53
Co II ratio	13	–	71	58
Case 13				
CS ratio	39	106	76	98
Co II ratio	37	–	73	92

Abbreviations: Co I, complex I; Co II, complex II; Co III, complex III; Co IV, complex IV; CS, citrate synthetase.
[a] Relative to mean CS and Co II of the normal controls.

lactate levels and muscle morphology can be used as a screening test, some confirmed patients were normal [10]. Third, genomic mutational analysis is difficult because MRC complexes are composed of 13 subunits encoded by mitochondrial DNA and over 70 subunits encoded by nuclear genes. In addition, nuclear genes are related to many assembly factors, membrane dynamics, nucleotide transport synthesis, and mitochondrial DNA replication and expression. Therefore, enzyme analysis still remains the most significant diagnostic tool. A definite diagnosis thus requires enzyme analysis [8].

In the present study, we performed enzyme analysis in frozen heart, frozen liver, and cultured fibroblasts. Eleven cases were supposed to be a probable diagnosis and two cases were supposed to be a possible diagnosis. However, it seemed unlikely that such a high proportion would have real MRC disorders. Did we have to take the effect of postmortem changes into consideration?

For forensic autopsy, organ specimens are often preserved in formaldehyde solution and sometimes frozen. These specimens are susceptible to postmortem changes and, therefore, correct enzyme analysis is hard to be performed. Based on the previous report that artifactual loss of complex II activity in autopsy samples preceded that of complex I and the data that complex II activity in the present study was maintained, this low complex I activity might be decreased before death. However, postmortem changes cannot be completely ruled out and this low complex I activity may not therefore be consistent with premortem activity.

We therefore analyzed activity in cultured fibroblasts. Cultured fibroblasts are not affected by postmortem changes and, therefore, reflect premortem information more accurately. In cultured fibroblasts, one case (case 5) of complex I activity met the major criteria and one case (case 13) of complex I activity met the minor criteria. In case 5, complex I activity was distinctively decreased. Sudan III staining of the case revealed hepatic steatosis, consistent with Reye-like syndrome. Reye-like syndrome is one of the characteristic features of MRC disorders [9]. We could therefore make a probable diagnosis (case 5) and a possible diagnosis (case 13) from metabolic autopsy with postmortem cultured fibroblasts.

Case 5 had hydrocephalia and case 13 was a low-birth-weight infant. However, neither was severe. Macroscopic examination did not reveal any abnormal appearance and microscopic examination showed no pathological findings except for steatosis. These cases might not have been identified without postmortem cultured fibroblasts. As with such cases, some MRC disorders reveal no clinical manifestation and no pathological characteristic. We believe it is important to perform metabolic autopsy with postmortem cultured fibroblasts when encountering SUDI cases.

We emphasized the advantage of metabolic autopsy with cultured fibroblasts. First, despite lacking obvious preceding symptoms, MRC disorders could be diagnosed. Second, cultured cells are the only method to retrieve premortem information from the deceased. Third, even frozen samples are affected by postmortem changes and may lead to a false positive diagnosis. However, we have to discuss the disadvantage. MRC disorders showed tissue specificity and the activity of cultured fibroblasts represent normal in some cases. Some of the low complex I activity in heart or liver could represent premortem MRC disorders despite normal activity in cultured fibroblasts. Thus, other molecular investigations may well be added to enzyme analysis. Recently, systematic gene analysis using next-generation sequencing has been reported for the diagnosis of patients with MRC disorders [17]. Further investigations are thus needed.

In conclusion, we detected one probable case and one possible case of MRC disorders among 13 Japanese cases of SUDI. MRC disorders are one of the important inherited metabolic disorders causing SUDI. We advocate metabolic autopsy with postmortem cultured fibroblasts in SUDI cases.

Acknowledgments

We would like to thank the Department of Pediatrics of Shimane University for acylcarnitine analysis. This study was partly supported by a grant from The Ministry of Health, Labour and Welfare of Japan and a grant of the Innovative Cell Biology by Innovative Technology (Cell Innovation Program) from the Ministry of Education, Culture, Sports, Science and Technology, Japan. The English used in this article was revised by Peter Todd.

References

[1] M.J. Bennett, S. Powell, Metabolic disease and sudden, unexpected death in infancy, Hum. Pathol. 25 (1994) 742–746.
[2] J.B. Lundemose, S. Kolvraa, N. Gregersen, E. Christensen, M. Gregersen, Fatty acid oxidation disorders as primary cause of sudden and unexpected death in infants and young children: an investigation performed on cultured fibroblasts from 79 children who died aged between 0–4 years, Mol. Pathol. 50 (1997) 212–217.
[3] R.G. Boles, E.A. Buck, M.G. Blitzer, M.S. Platt, T.M. Cowan, S.K. Martin, H. Yoon, J.A. Madsen, M. Reyes-Mugica, P. Rinaldo, Retrospective biochemical screening of fatty acid oxidation disorders in postmortem livers of 418 cases of sudden death in the first year of life, J. Pediatr. 132 (1998) 924–933.
[4] D.H. Chace, J.C. DiPerna, B.L. Mitchell, B. Sgroi, L.F. Hofman, E.W. Naylor, Electrospray tandem mass spectrometry for analysis of acylcarnitines in dried postmortem blood specimens collected at autopsy from infants with unexplained cause of death, Clin. Chem. 47 (2001) 1166–1182.
[5] R.L. Wilcox, C.C. Nelson, P. Stenzel, R.D. Steiner, Postmortem screening for fatty acid oxidation disorders by analysis of Guthrie cards with tandem mass spectrometry in sudden unexpected death in infancy, J. Pediatr. 141 (2002) 833–836.
[6] T. Yamamoto, H. Tanaka, H. Kobayashi, K. Okamura, T. Tanaka, Y. Emoto, K. Sugimoto, M. Nakatome, N. Sakai, H. Kuroki, S. Yamaguchi, R. Matoba, Retrospective review of Japanese sudden unexpected death in infancy: the importance of metabolic autopsy and expanded newborn screening, Mol. Genet. Metab. 102 (2011) 399–406.
[7] R. Luft, D. Ikkos, G. Palmieri, L. Ernster, B. Afzelius, A case of severe hypermetabolism of nonthyroid origin with a defect in the maintenance of mitochondrial respiratory control: a correlated clinical, biochemical, and morphological study, J. Clin. Invest. 41 (1962) 1776–1804.
[8] D. Skladal, J. Halliday, D.R. Thorburn, Minimum birth prevalence of mitochondrial respiratory chain disorders in children, Brain 126 (2003) 1905–1912.
[9] C. Arakawa, A. Endo, R. Kohira, Y. Fujita, T. Fuchigami, H. Mugishima, A. Ohtake, K. Murayama, M. Mori, R. Miyata, Y. Hatai, Liver-specific mitochondrial respiratory chain complex I deficiency in fatal influenza encephalopathy, Brain Dev. 34 (2012) 115–117.
[10] D.M. Kirby, M. Crawford, M.A. Cleary, H.H. Dahl, X. Dennett, D.R. Thorburn, Respiratory chain complex I deficiency: an underdiagnosed energy generation disorder, Neurology 52 (1999) 1255–1264.
[11] F.P. Bernier, A. Boneh, X. Dennett, C.W. Chow, M.A. Cleary, D.R. Thorburn, Diagnostic criteria for respiratory chain disorders in adults and children, Neurology 59 (2002) 1406–1411.
[12] K. Gibson, J.L. Halliday, D.M. Kirby, J. Yaplito-Lee, D.R. Thorburn, A. Boneh, Mitochondrial oxidative phosphorylation disorders presenting in neonates: clinical manifestations and enzymatic and molecular diagnoses, Pediatrics 122 (2008) 1003–1008.
[13] F. Valsecchi, W.J. Koopman, G.R. Manjeri, R.J. Rodenburg, J.A. Smeitink, P.H. Willems, Complex I disorders: causes, mechanisms, and development of treatment strategies at the cellular level, Dev. Disabil. Res. Rev. 16 (2010) 175–182.
[14] A. Munnich, P. Rustin, Clinical spectrum and diagnosis of mitochondrial disorders, Am. J. Med. Genet. 106 (2001) 4–17.
[15] M.J. Bennett, P. Rinaldo, The metabolic autopsy comes of age, Clin. Chem. 47 (2001) 1145–1146.
[16] A. Munnich, A. Rotig, D. Chretien, V. Cormier, T. Bourgeron, J.P. Bonnefont, J.M. Saudubray, P. Rustin, Clinical presentation of mitochondrial disorders in childhood, J. Inherit. Metab. Dis. 19 (1996) 521–527.
[17] S.E. Calvo, A.G. Compton, S.G. Hershman, S.C. Lim, D.S. Lieber, E.J. Tucker, A. Laskowski, C. Garone, S. Liu, D.B. Jaffe, J. Christodoulou, J.M. Fletcher, D.L. Bruno, J. Goldblatt, S. Dimauro, D.R. Thorburn, V.K. Mootha, Molecular diagnosis of infantile mitochondrial disease with targeted next-generation sequencing, Sci. Transl. Med. 4 (2012) 118ra10.

Journal of Chromatography B, 900 (2012) 24–31

Contents lists available at SciVerse ScienceDirect

Journal of Chromatography B

journal homepage: www.elsevier.com/locate/chromb

Detection of Δ^4-3-oxo-steroid 5β-reductase deficiency by LC–ESI-MS/MS measurement of urinary bile acids

Akina Muto[a], Hajime Takei[a], Atsushi Unno[a], Tsuyoshi Murai[b], Takao Kurosawa[b], Shoujiro Ogawa[c], Takashi Iida[c], Shigeo Ikegawa[d], Jun Mori[e], Akira Ohtake[f], Takayuki Hoshina[g], Tatsuki Mizuochi[h], Akihiko Kimura[h], Alan F. Hofmann[i], Lee R. Hagey[i], Hiroshi Nittono[a,*]

[a] *Junshin Clinic Bile Acid Institute, Haramachi, Meguro-ku, Tokyo 152-0011, Japan*
[b] *Faculty of Pharmaceutical Sciences, Health Sciences University of Hokkaido, Kanazawa, Ishikari-Tobetsu, Hokkaido 061-0293, Japan*
[c] *Department of Chemistry, College of Humanities & Sciences, Nihon University, Sakurajousui, Setagaya-ku, Tokyo 156-8550, Japan*
[d] *Faculty of Pharmaceutical Sciences, Kinki University, Kowakae, Higashi, Osaka 577-8502, Japan*
[e] *Department of Pediatrics, Kyoto Prefectural University of Medicine Graduate School of Medical Science, Kajii-cho, Kawaramachi Hirokoji, Kamigyo-ku, Kyoto 602-8566, Japan*
[f] *Department of Pediatrics, School of Medicine, Saitama Medical University, Moroyama, Iruma-gun, Saitama 350-0495, Japan*
[g] *Department of Pediatrics, Graduate School of Medical Sciences, Kyushu University, Maidashi, Higashi-ku, Fukuoka 812-8582, Japan*
[h] *Department of Pediatrics and Child Health, Kurume University School of Medicine, Asahi-machi, Kurume-shi, Fukuoka 830-0011, Japan*
[i] *Department of Medicine, University of California, San Diego, La Jolla, CA 92093-0063, USA*

ARTICLE INFO

Article history:
Received 5 January 2012
Accepted 18 May 2012
Available online 24 May 2012

Keywords:
Abnormal bile acid
Δ^4-3-Oxo-steroid 5β-reductase deficiency
Inborn errors of bile acid metabolism
Profile
LC–ESI-MS/MS
GC–MS

ABSTRACT

The synthesis of bile salts from cholesterol is a complex biochemical pathway involving at least 16 enzymes. Most inborn errors of bile acid biosynthesis result in excessive formation of intermediates and/or their metabolites that accumulate in blood and are excreted in part in urine. Early detection is important as oral therapy with bile acids results in improvement. In the past, these intermediates in bile acid biosynthesis have been detected in neonatal blood or urine by screening with FAB-MS followed by detailed characterization using GC–MS. Both methods have proved difficult to automate, and currently most laboratories screen candidate samples using LC–MS/MS. Here, we describe a new, simple and sensitive analytical method for the identification and characterization of 39 conjugated and unconjugated bile acids, including Δ^4-3-oxo- and $\Delta^{4,6}$-3-oxo-bile acids (markers for Δ^4-3-oxo-steroid 5β-reductase deficiency), using liquid chromatography-electrospray ionization tandem mass spectrometry (LC–ESI-MS/MS). In this procedure a concentrated, desalted urinary sample (diluted with ethanol) is injected directly into the LC–ESI-MS/MS, operated with ESI and in the negative ion mode; quantification is obtained by selected reaction monitoring (SRM). To evaluate the performance of our new method, we compared it to a validated method using GC–MS, in the analysis of urine from two patients with genetically confirmed Δ^4-3-oxo-steroid 5β-reductase deficiency as well as a third patient with an elevated concentration of abnormal conjugated and unconjugated Δ^4-3-oxo-bile acids. The Δ^4-3-oxo-bile acids concentration recovered in three patients with 5β-reductase deficiency were 48.8, 58.9, and 49.4 μmol/mmol creatinine, respectively by LC–ESI-MS/MS.

1. Introduction

Bile acids are biosynthesized from cholesterol in a process that utilizes multiple partially overlapping enzymatic pathways to make substantial changes to the steroid ring nucleus and side-chain, a process that utilizes a minimum of 16 enzymes [1]. Some of the first inborn errors in these pathways were detected nearly 30 years ago [2,3] by the detection of intermediates in the bile acid biosynthetic pathway. Since that time, inborn errors of bile acid formation involving isolated defects in most of the enzymes in the biosynthetic pathway have been reported [4]. However, such enzymatic defects are extremely rare. The most common genetic defect in bile acid biosynthesis appears to be Δ^4-3-oxo-steroid 5β-reductase deficiency, first described by Setchell et al. [5]. In children with defects in the gene or promoter region of Δ^4-3-oxo-steroid 5β-reductase (gene *AKR1D1*), the urinary bile acid profile contains 7α-hydroxy-3-oxo-4-cholenoic acid (as its glycine *m/z* 444 and taurine *m/z* 494 conjugates), as well as its 12α-dihydroxy-metabolite (again as glycine *m/z* 460 and taurine *m/z* 510 conjugates), as shown in Fig. 1. Chenodeoxycholic acid and cholic acid, the normal primary bile acids in man are nearly undetectable. However,

* Corresponding author at: Junshin Clinic Bile Acid Institute, 2-1-22, Haramachi, Meguro-ku, Tokyo 152-0011, Japan.
E-mail address: bile-res@eco.ocn.ne.jp (H. Nittono).

1570-0232/$ – see front matter © 2012 Elsevier B.V. All rights reserved.
http://dx.doi.org/10.1016/j.jchromb.2012.05.023

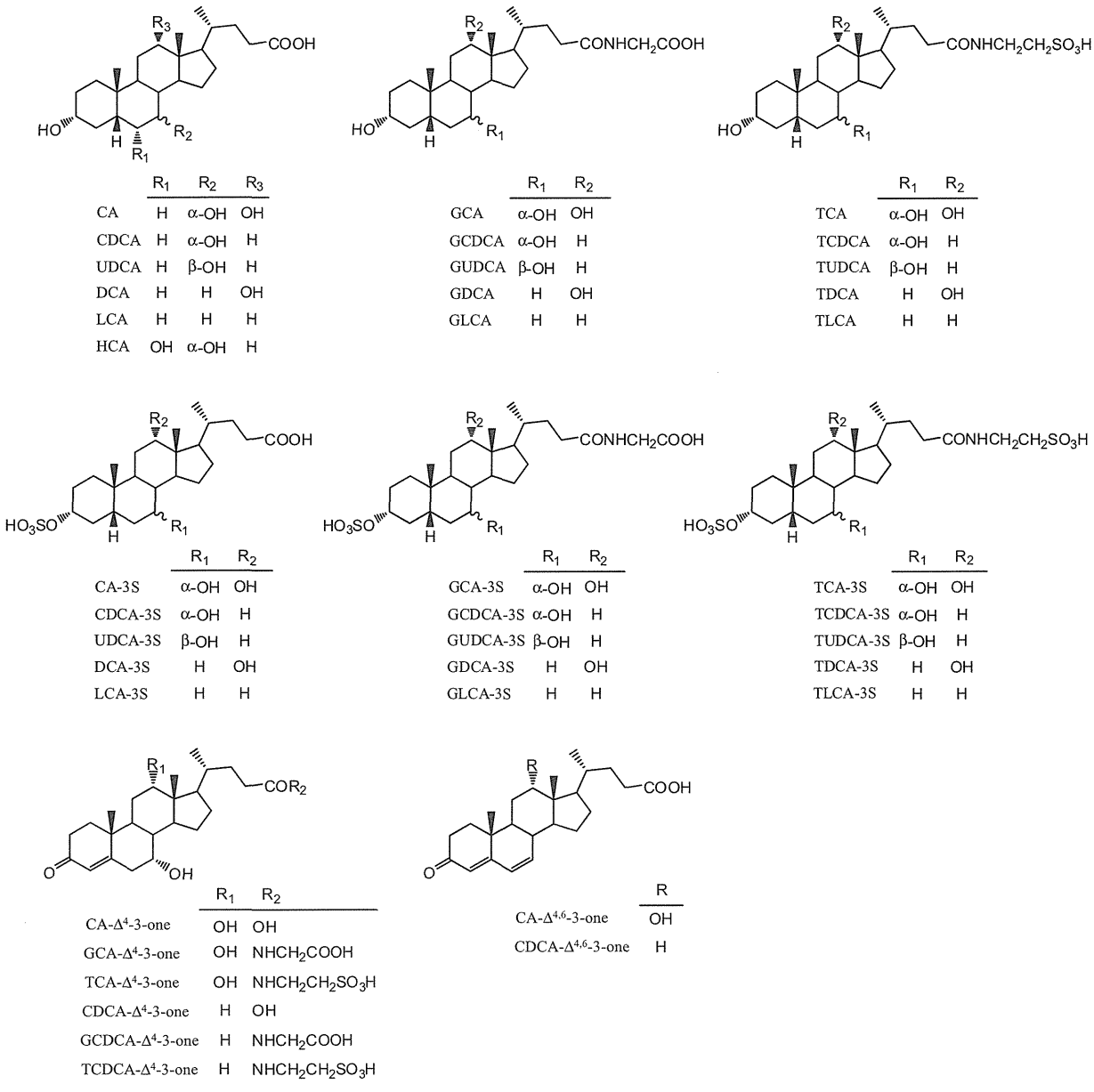

	R_1	R_2	R_3
CA	H	α-OH	OH
CDCA	H	α-OH	H
UDCA	H	β-OH	H
DCA	H	H	OH
LCA	H	H	H
HCA	OH	α-OH	H

	R_1	R_2
GCA	α-OH	OH
GCDCA	α-OH	H
GUDCA	β-OH	H
GDCA	H	OH
GLCA	H	H

	R_1	R_2
TCA	α-OH	OH
TCDCA	α-OH	H
TUDCA	β-OH	H
TDCA	H	OH
TLCA	H	H

	R_1	R_2
CA-3S	α-OH	OH
CDCA-3S	α-OH	H
UDCA-3S	β-OH	H
DCA-3S	H	OH
LCA-3S	H	H

	R_1	R_2
GCA-3S	α-OH	OH
GCDCA-3S	α-OH	H
GUDCA-3S	β-OH	H
GDCA-3S	H	OH
GLCA-3S	H	H

	R_1	R_2
TCA-3S	α-OH	OH
TCDCA-3S	α-OH	H
TUDCA-3S	β-OH	H
TDCA-3S	H	OH
TLCA-3S	H	H

	R_1	R_2
CA-Δ^4-3-one	OH	OH
GCA-Δ^4-3-one	OH	$NHCH_2COOH$
TCA-Δ^4-3-one	OH	$NHCH_2CH_2SO_3H$
CDCA-Δ^4-3-one	H	OH
GCDCA-Δ^4-3-one	H	$NHCH_2COOH$
TCDCA-Δ^4-3-one	H	$NHCH_2CH_2SO_3H$

	R
CA-$\Delta^{4,6}$-3-one	OH
CDCA-$\Delta^{4,6}$-3-one	H

Fig. 1. Chemical structures of unconjugated and conjugated bile acids used in this study.

because gene alterations cannot be found in the majority of patients excreting increased amounts of these urinary Δ^4-3-oxo-bile acids, it was eventually recognized that such abnormal bile acids could also accumulate and be excreted in urine in children with severely damaged liver functions [4]. This turned out to be the case for the first Japanese patient with possible Δ^4-3-oxo-steroid 5β-reductase deficiency [6].

The effects of an accumulation of potentially toxic bile acid intermediates, and the absence of completed bile acid structures, often results in life threatening cholestatic liver disease, and as a result, great emphasis has been placed on early diagnosis and treatment with replacement bile acid therapy. The most non-invasive means of obtaining a preliminary diagnosis is through the analysis of urine for altered bile acids. Most laboratories currently screen candidate samples using LC–ESI-MS/MS [7,8]. Urine samples are examined in the negative mode and searched for the dominant ions present between m/z 350 and m/z 700 using both the total ion current but also with selected precursor ion scans (parents of 74 for glycine conjugates; parents of 85 for glucuronide conjugates; parents of 97 for sulfate conjugates, and parents of 124 for taurine conjugates). A large number of methods based on LC–MS, with or without CID or multiple reaction monitoring (MRM), have been published, for a summary see Griffiths and Sjövall [9]. Many of these methods produce results that do not always agree with the more comprehensive ion exchange separation followed by GC–MS methods [10]. Recently, Griffiths & Sjövall [11] published a powerful LC–MS/MS method for the complete analysis of oxysterol metabolomes, however, this method is too sensitive and labor intensive for the routine analysis of neonatal urine samples.

Here we describe a new LC–MS/MS method for the analysis of human urinary bile acids. Our aims were to find a method that matched the results obtained by GC–MS methodology, to enable direct analysis of intact bile acid conjugates, to simplify sample preparation, and thus to develop an accurate analytical method that requires a minimum of time and labor. To evaluate the performance of our new method, we compared it to a validated GC–MS method, and then used both methods to analyze the urine from two patients with genetically confirmed Δ^4-3-oxo-steroid 5β-reductase

Table 1
LC–ESI-MS/MS date for unconjugated and conjugated bile acids examined.

Bile acid	RT (min)	Precursor ion (m/z)	Product ion (m/z)	CE (eV)	LOD (pmol/mL)	Correlation coefficient (r^2)
Saturated bile acids						
CA	31.1	407.2	343.2	33	0.50	0.9931
CDCA	34.6	391.3	373.2	32	8.79	0.9903
UDCA	29.5	391.3	373.2	32	14.31	0.9994
DCA	35.2	391.3	345.5	35	1.45	0.9929
LCA	37.9	375.2	357.2	33	21.54	0.9876
HCA	29.2	407.3	389.4	34	1.91	0.9954
GCA	29.5	464.3	74.0	39	0.08	0.9990
GCDCA	32.7	448.3	74.1	42	0.14	0.9995
GUDCA	27.6	448.3	74.1	42	0.19	0.9987
GDCA	33.6	448.3	74.1	42	0.12	0.9999
GLCA	36.0	432.3	74.1	39	0.03	0.9998
TCA	29.4	514.3	124.0	51	1.17	0.9944
TCDCA	32.5	498.3	124.0	51	0.34	0.9985
TUDCA	27.5	498.3	124.0	51	0.14	0.9922
TDCA	33.3	498.3	124.0	51	0.14	0.9933
TLCA	35.7	482.3	124.1	49	0.05	0.9973
CA-3S	24.5	487.3	97.0	46	0.03	0.9960
CDCA-3S	28.4	471.3	97.0	55	1.61	0.9974
UDCA-3S	23.2	471.3	97.0	55	0.30	0.9970
DCA-3S	28.8	471.3	97.0	55	0.64	0.9991
LCA-3S	31.7	455.3	97.0	44	0.01	0.9989
GCA-3S	22.1	271.7	97.0	41	0.05	0.9972
GCDCA-3S	25.5	263.7	97.0	40	0.03	0.9982
GUDCA-3S	20.3	263.7	97.0	40	0.03	0.9987
GDCA-3S	26.1	263.7	97.0	40	0.03	0.9990
GLCA-3S	28.5	255.7	97.0	40	0.37	0.9995
TCA-3S	22.2	296.7	97.0	38	0.04	0.9977
TCDCA-3S	25.4	288.7	97.0	39	0.03	0.9983
TUDCA-3S	20.4	288.7	97.0	39	0.03	0.9967
TDCA-3S	26.1	288.7	97.0	39	0.02	0.9975
TLCA-3S	28.4	280.7	97.0	37	1.13	0.9953
Unsaturated bile acids						
CA-Δ^4-3-one	23.8	403.3	123.1	39	0.09	0.9900
GCA-Δ^4-3-one	22.3	460.3	74.0	37	0.16	0.9992
TCA-Δ^4-3-one	22.4	510.3	124.1	50	0.33	0.9965
CDCA-Δ^4-3-one	29.0	387.3	369.4	27	0.83	0.9880
GCDCA-Δ^4-3-one	27.1	444.3	74.1	35	0.08	0.9980
TCDCA-Δ^4-3-one	27.0	494.3	124.0	44	0.76	0.9946
CA-$\Delta^{4,6}$-3-one	27.6	385.3	341.5	27	0.99	0.9822
CDCA-$\Delta^{4,6}$-3-one	33.2	369.3	325.5	28	0.39	0.9859

RT, retention time; CE, collision energy; LOD, limit of detection (S/N = 5).

deficiency as well as from a third patient with an elevated concentration of abnormal conjugated and unconjugated Δ^4-3-oxo-bile acids.

2. Experimental procedure

2.1. Materials and reagents

Authentic reference bile acids (see Appendix A) used in this study were as follows: cholic acid (CA), glycocholic acid (GCA), taurocholic acid (TCA), chenodeoxycholic acid (CDCA), glycochenodeoxycholic acid (GCDCA), taurochenodeoxycholic acid (TCDCA), ursodeoxycholic acid (UDCA), glycoursodeoxycholic acid (GUDCA), tauroursodeoxycholic acid (TUDCA), lithocholic acid (LCA), glycolithocholic acid (GLCA), taurolithocholic acid (TLCA), deoxycholic acid (DCA), taurodeoxycholic acid (TDCA) and hyocholic acid (HCA) were purchased from Sigma Chemicals (St. Louis, MO, USA). [2,2,4,4-d_4]-CA (d_4-CA, internal standard (IS) for unconjugated bile acids), [2,2,4,4-d_4]-GCA (d_4-GCA, IS for glycine conjugated bile acids), and [2,2,4,4-d_4]-TCA (d_4-TCA, IS for taurine conjugated and double conjugated bile acids) were obtained from CDD Isotopes Inc. (Quebec, Canada). The 3-sulfates for the following bile acids: CA, CDCA, UDCA, DCA, LCA, GCA, GCDCA, GUDCA, GDCA, GLCA, TCA, TCDCA, TUDCA, TDCA, and TLCA were synthesized by a previously reported method [12,13]. Unsaturated bile acids with the Δ^4-3-one configuration in the steroid nucleus for CA, GCA, TCA, CDCA, GCDCA, TCDCA, and for the $\Delta^{4,6}$-3-one for CA, and CDCA were synthesized by a previously reported method [14]. In this paper, we have used semi-trivial nomenclature for the Δ^4-3-one and $\Delta^{4,6}$-3-one derivatives of the common bile acids by using the abbreviation for the saturated compound. Ethanol, methanol, and water were of HPLC grade, ammonium acetate was analytical grade, and all were purchased from Kanto Chemical Co., Inc. (Tokyo, Japan).

2.2. Preparation of standards

Individual stock solutions of bile acids were prepared separately at 10 μmol/mL in ethanol and the stock solutions were stored at −20 °C. These solutions were mixed in equal amounts for the analysis of unknown samples, and five point calibration standard solutions (30, 100, 300, 1000, 3000 pmol/mL) were prepared in 50% ethanol. The calibration standard solutions were stable in analytical glass vials for 4 weeks at 4 °C.

2.3. Urine specimens

Urine samples used for the present analysis were as follows: urines from two patients with 5β-reductase deficiency (as determined by genetic diagnosis, case 2 patient was receiving UDCA); urine from a patient with 5β-reductase deficiency (as determined by urinary bile acids analysis and clinical diagnosis); urine from 9 healthy children (ages 2–3 years); and urine from 5 healthy

Table 2
Recovery test of unconjugated and conjugated bile acids examined by LC–ESI-MS/MS.

Bile acids	100 pmol/mL Recovery (n = 5, %)			1000 pmol/mL Recovery (n = 5, %)		
	Average	(Range)	R.S.D. (%)	Average	(Range)	R.S.D. (%)
Saturated bile acids						
CA	90.6	(87.0–94.8)	3.2	105.6	(86.5–114.7)	10.6
CDCA	91.6	(88.9–97.3)	3.8	107.8	(93.5–120.0)	11.9
UDCA	77.2	(67.0–95.6)	14.1	106.9	(82.8–120.0)	13.8
DCA	91.1	(85.9–95.7)	4.1	106.8	(85.5–117.9)	12.0
LCA	76.5	(70.0–85.4)	8.8	104.7	(96.1–112.5)	5.9
HCA	87.0	(83.2–93.1)	4.2	106.1	(88.0–118.0)	11.1
GCA	104.3	(98.3–106.4)	3.3	91.9	(82.9–108.4)	10.6
GCDCA	101.3	(98.8–103.7)	2.2	93.0	(86.4–109.6)	10.3
GUDCA	100.5	(96.4–104.1)	3.2	89.8	(82.3–109.0)	12.1
GDCA	98.4	(95.0–103.8)	8.2	89.7	(83.3–109.0)	12.0
GLCA	100.0	(95.5–106.2)	4.7	86.7	(83.5–94.0)	5.1
TCA	102.4	(97.4–104.2)	8.9	94.2	(88.9–99.5)	4.6
TCDCA	94.1	(92.2–99.0)	3.0	103.4	(94.8–111.0)	6.0
TUDCA	91.5	(84.0–99.8)	7.2	97.1	(86.4–107.6)	9.5
TDCA	100.9	(89.8–111.4)	7.6	95.2	(89.7–101.6)	5.0
TLCA	97.3	(90.6–100.7)	4.3	99.6	(95.4–105.3)	3.8
CA-3S	101.2	(98.2–003.8)	2.2	97.6	(89.1–104.6)	6.8
CDCA-3S	98.1	(95.5–102.1)	2.7	100.2	(92.7–109.7)	7.2
UDCA-3S	98.3	(94.0–103.2)	4.3	96.2	(89.1–105.8)	6.8
DCA-3S	101.6	(96.9–104.6)	3.2	118.8	(112.8–123.9)	3.5
LCA-3S	98.9	(95.0–102.8)	3.3	98.7	(91.6–103.7)	5.6
GCA-3S	99.3	(96.0–104.3)	3.4	101.2	(94.0–109.8)	6.3
GCDCA-3S	103.2	(98.4–106.7)	3.5	95.3	(88.1–106.2)	7.8
GUDCA-3S	101.1	(97.5–103.5)	2.9	100.8	(88.7–115.0)	9.3
GDCA-3S	103.2	(101.2–104.6)	1.3	106.2	(99.8–108.5)	3.4
GLCA-3S	99.8	(93.6–104.9)	5.6	109.1	(101.0–114.6)	5.2
TCA-3S	100.8	(98.8–103.8)	2.3	102.9	(95.7–112.2)	6.6
TCDCA-3S	98.2	(95.0–99.8)	1.9	103.0	(94.9–110.1)	6.6
TUDCA-3S	99.4	(96.8–102.6)	2.9	94.6	(92.1–98.7)	2.9
TDCA-3S	99.5	(95.4–104.3)	4.1	101.6	(92.3–110.5)	7.6
TLCA-3S	99.5	(96.3–103.0)	2.9	107.4	(99.1–117.9)	6.6
Unsaturated bile acids						
CA-Δ^4-3-one	85.0	(81.8–93.1)	4.4	105.9	(84.2–116.4)	11.9
GCA-Δ^4-3-one	100.1	(96.1–105.6)	3.6	88.2	(79.1–110.1)	14.2
TCA-Δ^4-3-one	94.7	(84.8–103.9)	8.7	94.1	(79.1–105.1)	11.9
CDCA-Δ^4-3-one	92.2	(89.9–94.7)	2.5	104.2	(88.1–112.7)	9.3
GCDCA-Δ^4-3-one	99.3	(96.9–100.9)	1.6	87.7	(81.5–105.4)	11.4
TCDCA-Δ^4-3-one	99.3	(95.1–104.5)	4.0	94.5	(86.5–98.4)	5.1
CA-$\Delta^{4,6}$-3-one	91.3	(87.0–96.0)	4.5	118.0	(96.3–128.3)	11.0
CDCA-$\Delta^{4,6}$-3-one	94.3	(89.4–99.5)	4.1	113.1	(88.7–121.9)	12.4

children (ages 6–8 months). All urine samples were stored at −25 °C until the pretreatment for analysis.

2.4. Sample preparation

For the LC–ESI-MS/MS analysis, 0.05 mL of the urine samples was used for analysis. 0.45 mL of 50% ethanol and IS, 0.5 mL, containing (d_4-CA, d_4-GCA and d_4-TCA 200 pmol/mL in 50% ethanol), was added to the urine. Precipitated solids were moved by filtration through a 0.45 μm millipore filter (Millex®-LG, Billerica, MA, USA). A 10 μL aliquot of the above filtrate was injected directly into the LC–ESI-MS/MS instrument.

2.5. LC–ESI-MS/MS conditions

The LC–ESI-MS/MS system consisted of a TSQ Quantum Discovery Max mass spectrometer (Thermo Fisher Scientific, San Jose, CA, USA) equipped with an ESI probe and Surveyor HPLC system (Thermo Fisher Scientific). A trapping column, Hypersil GOLD column (50 mm × 2.1 mm I.D., 5 μm of particle size; Thermo Fisher Scientific) and a chromatographic separation column, Inertsil Sustain C18 column (150 mm × 2.1 mm I.D., 3 μm particle size; G&L Science, Tokyo, Japan) were employed at 40 °C. A trapping column *via* a column-switching valve was used for the on-line desalting and concentration of urine specimens [15]. After injection of the sample solution, the trapping column was washed with 5 mM ammonium acetate (AA) for 5.5 min at flow rate of 0.1 mL/min, eluted with ethanol, and then transferred into the separation column. A mixture of 5 mM ammonium acetate, ethanol and methanol was used as the eluent, and the separation carried out by linear gradient elution at a flow rate of 0.2 mL/min. The mobile phase composition of ethanol and methanol was gradually changed as follows: ammonium acetate for 3.5 min, ammonium acetate–ethanol (9:1, v/v) for 3.5–4 min, ammonium acetate–ethanol (7:3, v/v) for 4–10 min, ammonium acetate–ethanol–methanol (57:10:33, v/v/v) for 10–16 min, ammonium acetate–ethanol–methanol (2:3:95, v/v/v) for 16–43 min, and then ammonium acetate–ethanol–methanol (2:3:95, v/v/v) for 43–47 min; the column was re-equilibrated for 5 min. Altogether, the total run time was 52 min.

To operate the LC–ESI-MS/MS, the spray voltage and vaporizer temperature were set at 3500 V and 330 °C, respectively. The sheath and auxiliary gas (nitrogen) pressure were set at 50 and 10 arbitrary units, respectively, and the ion transfer capillary temperature was carried out at 330 °C. The collision gas (argon) pressure and the collision energy were kept at 1.3 mm Torr and 27–55 eV, respectively, all in the negative ion mode.

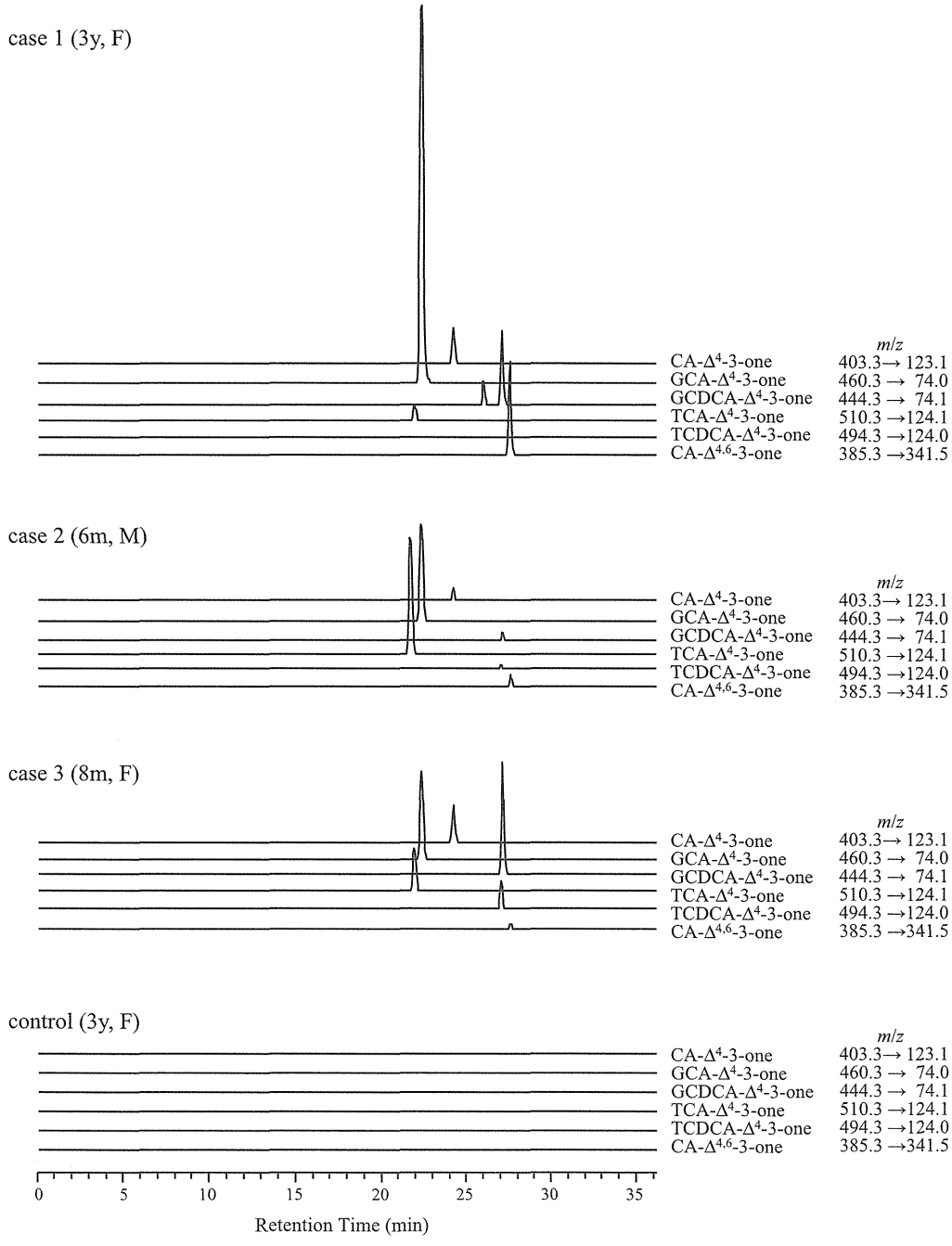

Fig. 2. Selected reaction monitoring chromatograms of urinary bile acids in three patients with 5β-reductase deficiency, as well as healthy control, by LC–ESI-MS/MS.

2.6. Validation of LC–ESI-MS/MS methodology

To characterize the LC–ESI-MS/MS method, we examined specific product ions generated by selecting parent ions and altering the ESI collision energy. Initially, a simultaneous analysis of unconjugated and conjugated bile acids found that a portion of the bile acids were quite sensitive to detection in the positive mode; however, overall, the negative mode was found to be much more appropriate for the measurement of all bile acids as has been reported previously [8]. For the detection of parent ions by ESI, it was possible to select two types of negative ion charges-$[M-H]^-$ for unconjugated bile acids, *N*-acylamidated bile acids and nonamidated bile acid 3-sulfates and $[M-2H]^{2-}$ for the *N*-acylamidated bile acid 3-sulfates [13]. Optimal conditions to conduct the selected reaction monitoring (SRM) were established by the collision-induced dissociation (CID) experiments carried out for each bile acid, and the most suitable collision energy determined by observing the characteristic product ions. The product ions of *N*-acylamidated conjugates were best detected at *m/z* 74.0 (glycine conjugates) and 124.0 (taurine conjugates); sulfated bile acids were best detected at *m/z* 97.0.

2.7. GC–MS analysis

For the GC–MS analysis, an aliquot of 0.5 mL of urine samples before dried and derivatized as a methyl ester-dimethylethyl silyl ether product, as previously described [16]. Ten unconjugated bile acids (CA, CDCA, UDCA, DCA, LCA, HCA, CA-Δ^4-3-one, CDCA-Δ^4-3-one, CA-$\Delta^{4,6}$-3-one and CDCA-$\Delta^{4,6}$-3-one) were used for the GC–MS analysis, which was performed on a Hewlett

Table 3
Urinary bile acid profile in three patients with 5β-reductase deficiency and healthy controls by LC–ESI-MS/MS.

	Healthy control (2–3y, $n=9$)	Healthy control (6–8m, $n=5$)	Case 1 (3y)	Case 2[a] (6m)	Case 3 (8m)
Saturated bile acids					
CA	–	–	–	–	–
CDCA	–	–	–	–	–
UDCA	–	–	–	–	–
DCA	–	–	–	–	–
LCA	–	–	–	–	–
HCA	–	–	–	–	–
GCA	–	–	–	–	–
GCDCA	–	–	–	–	–
GUDCA	–	–	–	0.99	–
GDCA	–	–	–	–	–
GLCA	–	–	–	–	–
TCA	–	–	–	–	
TCDCA	–	–	–	–	
TUDCA	–	–	–	–	–
TDCA	–	–	–	–	–
TLCA	–	–	–	–	–
CA-3S	–	–	–	–	–
CDCA-3S	–	–	–	–	–
UDCA-3S	–	–	–	–	–
DCA-3S	–	–	–	–	–
LCA-3S	–	–	–	–	–
GCA-3S	–	–	–	1.51	0.10
GCDCA-3S	0.19 ± 0.14	0.31 ± 0.13	–	–	–
GUDCA-3S	–	–	–	1.64	–
GDCA-3S	0.11 ± 0.16	–	–	–	–
GLCA-3S	0.02 ± 0.04	–	–	–	–
TCA-3S	–	–	–	–	–
TCDCA-3S	0.02 ± 0.03	0.11 ± 0.05	–	–	0.16
TUDCA-3S		–	–	1.10	
TDCA-3S		–	–	–	
TLCA-3S	0.00 ± 0.01	–	–	–	–
Unsaturated bile acids					
CA-Δ^4-3-one	–	–	1.59	0.82	2.58
GCA-Δ^4-3-one	–	–	40.12	22.64	18.23
TCA-Δ^4-3-one	–	–	2.91	33.26	11.85
CDCA-Δ^4-3-one	–	–	–	–	–
GCDCA-Δ^4-3-one	–	–	3.97	1.18	10.38
TCDCA-Δ^4-3-one	–	–	0.17	1.02	6.39
CA-$\Delta^{4,6}$-3-one	–	–	1.10	0.54	0.38
CDCA-$\Delta^{4,6}$-3-one	–	–	–	–	–

Unit: μmol/mmol Cr; Cr, creatinine.
[a] Case 2 patient was receiving UDCA.

Packard 5890 gas chromatograph (Agilent, Santa Clara CA, USA) and Hewlett Packard 5973 mass selective detector instrument (Agilent, Santa Clara CA, USA). A fused-silica capillary column bonded with methylsilicon, DB5MS (30 m × 0.25 mm I.D., 0.25 μm film thickness; Agilent) was used to separate the derivatized bile acids. A carrier gas (helium) of flow rate was 1.4 mL/min. was used, and the column temperature was held at 170 °C for 2 min and then ramped at 10 °C/min until 230 °C ramped again at 3 °C/min. up to 310 °C. Mass spectra were recorded at 70 eV for the ionization energy and at 250 °C for the ion source temperature.

2.8. Method validation

2.8.1. Recoveries of bile acids and ISs during pretreatment

The recoveries of bile acids were calculated from the peak area ratios of unconjugated bile acids/d_4-CA, glycine conjugated bile acids/d_4-GCA, and taurine conjugated and double conjugated bile acids/d_4-TCA, respectively, in sample A and B as described below. The recoveries of ISs were calculated from the peak area ratios of d_4-CA/CA, d_4-GCA/GCA, and d_4-TCA/TCA in sample A and B as described below.

Sample A: the blank urine (0.05 mL) spiked with 39 reference bile acids (100 pmol) was pretreated. After addition of ISs (100 pmol each) to this pretreated urine, the resulting sample was subjected to LC–ESI-MS/MS.

Sample B: the blank urine (0.05 mL) spiked with 39 reference bile acids (1000 pmol) was pretreated. After addition of ISs (100 pmol each) to this pretreated urine, the resulting sample was subjected to LC–ESI-MS/MS.

2.8.2. Reproducibility

The reproducibility was assessed by determining two urine samples at different concentration levels ($n=5$ for each sample) and determined as the relative standard deviation (R.S.D.%).

2.8.3. Assay accuracy (analytical recovery)

50% ethanol (0.45 mL) was added to the urine (the spiked concentrations of bile acids were 100 and 1000 pmol, respectively). After the addition of ISs (100 pmol each), each of the resulting samples were pretreated and analyzed by LC–MS/MS. The assay accuracy (analytical recovery) of bile acids was defined as $F/(F_0+A)\times 100\%$, where F is the concentration of bile acids in the spiked sample, F_0 is the concentration of bile acids in the unspiked sample and A is the spiked concentration.

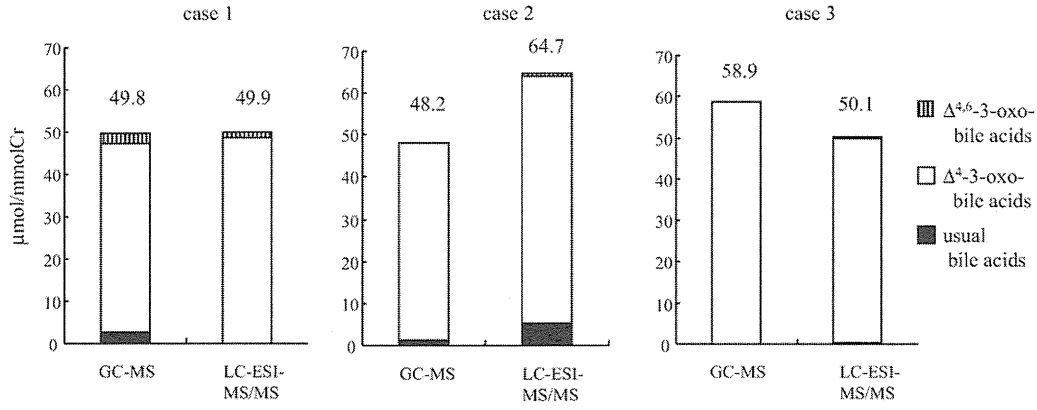

Fig. 3. Comparison of urinary bile acids levels by GC/MS and LC–ESI-MS/MS. Levels shown by GC/MS are the concentration of total bile acids following deconjugation by enzymatic hydrolysis. The results using LC–ESI-MS/MS are the concentration of total unconjugated bile acids combined with their glycine, taurine, and unconjugated bile acid sulfates as well as the *N*-acylamidates of the bile acid sulfates.

3. Results

Fig. 1 shows the chemical structures of the 39 variants of unconjugated and conjugated C_{24} bile acids examined in this study, which include the unconjugated bile acids, *N*-acylamidate conjugates with glycine or taurine at C-24 in the side chain, as well as the C-3 sulfated bile acids in unconjugated and *N*-acylamidated forms. For the initial LC–ESI-MS/MS analysis, we examined the optimum conditions for generating specific product ions arising from the respective parent ions (protonated molecule $[M+H]^+$ or deprotonated molecule $[M-H]^-$) in both the positive and negative ion charge modes. Most of the bile acids showed a high sensitivity and selectivity in the negative mode. Tube lens offset voltage and collision energy of each bile acid, and their conjugates under negative-ion ESI-MS/MS were optimized by directly injecting the standard solution. The most abundant transitions that could be used for monitoring ion are listed in Table 1. The chromatographic conditions, especially the composition of mobile phase, were optimized through several trials. When using an Inertsil Sustain C18 column and a linear gradient elution of ammonium acetate for 3.5 min, ammonium acetate–ethanol (9:1, v/v) for 3.5–4 min, ammonium acetate–ethanol (7:3, v/v) for 4–10 min, ammonium acetate–ethanol–methanol (57:10:33, v/v/v) for 10–16 min, ammonium acetate–ethanol–methanol (2:3:95, v/v/v) for 16–43 min, and then ammonium acetate–ethanol–methanol (2:3:95, v/v/v) for 43–47 min at a flow rate of 0.2 mL/min, satisfactory separation of each bile acid was achieved, and the chromatographic run time was 52 min; retention times and transitions used in SRM for bile acids are given in Table 1. Calibration graphs were then constructed by plotting the peak-area ratio of each bile acid to those of [2,2,4,4-d_4]-CA (IS for unconjugated bile acids), [2,2,4,4-d_4]-GCA (IS for glycine conjugated bile acids), and [2,2,4,4-d_4]-TCA (IS for taurine conjugated and double conjugated bile acids) *versus* the weights of the bile acid. The response was linear with correlation coefficient (r^2) of 0.9822–0.9999 within the range of 30–3000 pmol/mL. The assay reproducibility was examined by 5 repetitive measurement of healthy volunteer's, which contained different concentrations of bile acid. The assay of R.S.D for all the bile acids was less than 14.2%. The assay accuracy was evaluated as the analytical recovery. As shown in Table 2, satisfactory recovery rates ranging from 76.5 to 118.8% were obtained. These data indicate that the present method is highly reproducible and accurate.

Having validated the method for LC–ESI-MS/MS, we then examined the urinary bile acid profiles in a control patient, and in three patients with 5β-reductase deficiency. The results are shown in Fig. 2, in which the abnormal Δ^4-3-oxo bile acids stand out prominently in the three 5β-reductase deficient patients (48.8 μmol/mmol creatinine (Cr), case 1; 58.9 μmol/mmol Cr, case 2; and 49.4 μmol/mmol Cr, case 3), and are completely absent in the normal control. The results of a quantitative determination of total urinary bile acids for two controls and the three 5β-reductase patients are shown in Table 3.

We then analyzed the urines from the three 5β-reductase patients using a validated GC–MS method, and compared the GC–MS results to the data obtained using our LC–ESI-MS/MS methodology. As shown in Fig. 3, both methods gave near identical results, as both the GC–MS and LC–ESI-MS/MS could detect Δ^4-3-oxo and $\Delta^{4,6}$-3-oxo bile acids in these urine samples in a similar proportion. In Fig. 3, the total bile acid concentration recovered in cases 1–3 was 49.8, 48.2, and 58.9 μmol/mmol Cr (respectively) by GC–MS, and 49.9, 64.7, and 50.1 μmol/mmol Cr (respectively) by LC–ESI-MS/MS. Values for urine samples from control subjects done under identical conditions yielded less than 1% Δ^4-3-oxo and $\Delta^{4,6}$-3-oxo bile acids (data not shown).

4. Discussion

The method reported describes a time and labor saving LC–ESI-MS/MS method for human urine that requires only a quick dilution step with alcohol, filtration through a standard 0.45 μm millipore filter, and direct injection into the instrument. In comparison with previously published methods for FAB-MS [17] and GC–MS [18,19], our method is able to separate and identify 39 conjugated and unconjugated bile acids found in urine. In addition, whereas other LC–ESI-MS/MS methods produce results that are often not in accordance with validated GC–MS methods, results obtained with our methodology agree quite well with those obtained by GC–MS. A clear advantage of our method over GC–MS is its ability to detect and quantify the bile acid conjugates and distinguish them from unconjugated bile acids. Thus, our method shows that the Δ^4-3-one bile acids were present as taurine and glycine conjugates. In contrast, the GC–MS method requires a prior enzymatic deconjugation step and thus does not provide such information.

The life-threatening severity of inborn errors of bile acids metabolism, and their need for early detection, has led to a proliferation of non-invasive screening methods. In patients either with confirmed 5β-reductase deficiency, or with severe liver disease, the output of normal bile acids is suppressed and bile acid precursors appear in the urine. Current treatment protocols call for the oral administration of primary bile acids in patients with inborn errors of bile acid biosynthesis, and following the response to treatment by monitoring tests of liver injury. Our quantitative method should

enable a real-time monitoring of the effects of the course of treatment, by following the gradual reduction and disappearance of bile acid precursors from the urine.

Appendix A.

Abbreviations and the corresponding trivial names of unconjugated, *N*-acylamidated (with glycine or taurine), and sulfated bile acids used in this study.

CA	Cholic acid
CDCA	Chenodeoxycholic acid
UDCA	Ursodeoxycholic acid
DCA	Deoxycholic acid
LCA	Lithocholic acid
HCA	Hyocholic acid
GCA	Glycocholic acid
GCDCA	Glycochenodeoxycholic acid
GUDCA	Glycoursodeoxycholic acid
GDCA	Glycodeoxycholic acid
GLCA	Glycolithocholic acid
TCA	Taurocholic acid
TCDCA	Taurochenodeoxycholic acid
TUDCA	Tauroursodeoxycholic acid
TDCA	Taurodeoxycholic acid
TLCA	Taurolithocholic acid
CA-3S	Cholic acid 3-sulfate
CDCA-3S	Chenodeoxycholic acid 3-sulfate
UDCA-3S	Ursodeoxycholic acid 3-sulfate
DCA-3S	Deoxycholic acid 3-sulfate
LCA-3S	Lithocholic acid 3-sulfate
GCA-3S	Glycocholic acid 3-sulfate
GCDCA-3S	Glycochenodeoxycholic acid 3-sulfate
GUDCA-3S	Glycoursodeoxycholic acid 3-sulfate
GDCA-3S	Glycodeoxycholic acid 3-sulfate
GLCA-3S	Glycolithocholic acid 3-sulfate
TCA-3S	Taurocholic acid 3-sulfate
TCDCA-3S	Taurochenodeoxycholic acid 3-sulfate
TUDCA-3S	Tauroursodeoxycholic acid 3-sulfate
TDCA-3S	Taurodeoxycholic acid 3-sulfate
TLCA-3S	Taurolithocholic acid 3 sulfate
CA-Δ^4-3-one	7α,12α-Dihydroxy-3-oxo-4-cholenoic acid
GCA-Δ^4-3-one	7α,12α-Dihydroxy-3-oxo-4-cholen-24-oic acid *N*-(carboxymethyl)amide
TCA-Δ^4-3-one	7α,12α-Dihydroxy-3-oxo-4-cholen-24-oic acid *N*-(2-sulfoethyl)amide
CDCA-Δ^4-3-one	7α-Hydroxy-3-oxo-4-cholen-24-oic acid
GCDCA-Δ^4-3-one	7α-Hydroxy-3-oxo-4-cholen-24-oic acid *N*-(carboxymethyl)amide
TCDCA-Δ^4-3-one	7α-Hydroxy-3-oxo-4-cholen-24-oic acid *N*-(2-sulfoethyl)amide
CA-$\Delta^{4,6}$-3-one	12α-Hydroxy-3-oxo-4,6-choladien-24-oic acid
CDCA-$\Delta^{4,6}$-3-one	3-Oxo-4,6-choladien-24-oic acid

References

[1] D.W. Russell, J. Lipid Res. 50 (2009) S120.
[2] H. Eyssen, G. Parmentier, F. Compernolle, J. Boon, E. Eggermont, Biochim. Biophys. Acta 273 (1972) 212.
[3] R.F. Hanson, J.N. Isenberg, G.C. Williams, D. Hachey, P. Szczepanik, P.D. Klein, H.L. Sharp, J. Clin. Invest. 56 (1975) 577.
[4] P.T. Clayton, J. Inherit. Metab. Dis. 34 (2011) 593.
[5] K.D. Setchell, F.J. Suchy, M.B. Welsh, L. Zimmer-Nechemias, J. Heubi, W.F. Balistreri, J. Clin. Invest. 82 (1988) 2148.
[6] A. Kimura, K.H. Kondo, K.I. Okuda, S. Higashi, M. Suzuki, T. Kurosawa, M. Tohma, T. Inoue, A. Nishiyori, M. Yoshino, H. Kato, T. Setoguchi, Eur. J. Pediatr. 157 (1998) 386.
[7] K.A. Mills, I. Mushtaq, A.W. Johnson, P.D. Whitfield, P.T. Clayton, Pediatr. Res. 43 (1998) 361.
[8] I.M. Yousef, S. Perwaiz, T. Lamireau, B. Tuchweber, Med. Sci. Monit. 9 (2003) MT21.
[9] W.J. Griffiths, J. Sjövall, J. Lipid Res. 51 (2010) 23.
[10] J. Sjövall, W.J. Griffiths, K.D. Setchell, N. Mano, J. Goto, in: H.L. Makin, D.B. Gower (Eds.), Steroid Analysis, Springer, 2010, p. 837.
[11] W.J. Griffiths, J. Sjövall, Biochem. Biophys. Res. Commun. 396 (2010) 80.
[12] J. Goto, H. Kato, F. Hasegawa, T. Nambara, Chem. Pharm. Bull. (Tokyo) 27 (1979) 1402.
[13] T. Goto, K.T. Myint, K. Sato, O. Wada, G. Kakiyama, T. Iida, T. Hishinuma, N. Mano, J. Goto, J. Chromatogr. B 846 (2007) 69.
[14] I. Björkhem, H. Danielsson, C. Issidorides, A. Kallner, Acta Chem. Scand. 19 (1965) 2151.
[15] N. Kishi, N. Mano, N. Asakawa, Anal. Sci. 17 (2001) 709.
[16] M. Suzuki, T. Murai, T. Yoshimura, A. Kimura, T. Kurosawa, M. Tohma, J. Chromatogr. B 693 (1997) 11.
[17] F.J. Suchy, R.J. Sokol, W.F. Balistereri (Eds.), Liver Disease in Children, Cambridge University Press, New York, 2007, p. 736.
[18] A. Unno, H. Nittono, H. Takei, T. Tawa, A. Tokita, Y. Yamashiro, M. Matsumoto, A. Kimura, T. Murai, T. Kurosawa, M. Tohma, Jpn. J. Pediatr. Gastroenterol. Hepatol. Nutr. 14 (2000) 25 (in Japanese).
[19] H. Nittono, H. Takei, A. Unno, A. Kimura, T. Shimizu, T. Kurosawa, M. Tohma, M. Une, Pediatr. Int. 51 (2009) 535.

Anal Bioanal Chem (2013) 405:1345–1351
DOI 10.1007/s00216-012-6532-3

ORIGINAL PAPER

Intracellular in vitro probe acylcarnitine assay for identifying deficiencies of carnitine transporter and carnitine palmitoyltransferase-1

Jamiyan Purevsuren · Hironori Kobayashi · Yuki Hasegawa · Kenji Yamada · Tomoo Takahashi · Masaki Takayanagi · Toshiyuki Fukao · Seiji Fukuda · Seiji Yamaguchi

Received: 24 July 2012 / Revised: 10 October 2012 / Accepted: 30 October 2012 / Published online: 10 November 2012

Abstract Mitochondrial fatty acid oxidation (FAO) disorders are caused by defects in one of the FAO enzymes that regulates cellular uptake of fatty acids and free carnitine. An in vitro probe acylcarnitine (IVP) assay using cultured cells and tandem mass spectrometry is a tool to diagnose enzyme defects linked to most FAO disorders. Extracellular acylcarnitine (AC) profiling detects carnitine palmitoyltransferase-2, carnitine acylcarnitine translocase, and other FAO deficiencies. However, the diagnosis of primary carnitine deficiency (PCD) or carnitine palmitoyltransferase-1 (CPT1) deficiency using the conventional IVP assay has been hampered by the presence of a large amount of free carnitine (C0), a key molecule deregulated by these deficiencies. In the present study, we developed a novel IVP assay for the diagnosis of PCD and CPT1 deficiency by analyzing intracellular ACs. When exogenous C0 was reduced, intracellular C0 and total AC in these deficiencies showed specific profiles clearly distinguishable from other FAO disorders and control cells. Also, the ratio of intracellular to extracellular C0 levels showed a significant difference in cells with these deficiencies compared with control. Hence, intracellular AC profiling using the IVP assay under reduced C0 conditions is a useful method for diagnosing PCD or CPT1 deficiency.

Keywords Fatty acid oxidation · Carnitine cycle disorder · Acylcarnitine profile · ESI-MS/MS

J. Purevsuren · H. Kobayashi · Y. Hasegawa · K. Yamada · T. Takahashi · S. Fukuda · S. Yamaguchi (✉)
Department of Pediatrics, Shimane University School of Medicine, 89-1 Enya,
Izumo, Shimane 693-8501, Japan
e-mail: seijiyam@med.shimane-u.ac.jp

M. Takayanagi
Division of Metabolism, Chiba Children's Hospital,
Chiba 266-0007, Japan

T. Fukao
Department of Pediatrics, Graduate School of Medicine,
Gifu University,
Gifu, Gifu 501-1194, Japan

T. Fukao
Medical Information Sciences Division, United Graduate School of Drug Discovery and Medical Information Sciences,
Gifu University,
Gifu, Gifu 501-1194, Japan

J. Purevsuren
Medical Genetics Laboratory,
National Center for Maternal and Child Health,
Khuvisgalchdyn street, Bayangol district,
Ulaanbaatar 210624, Mongolia

Introduction

L-Carnitine plays an essential role in the transfer and activation of long-chain fatty acids across the outer and inner mitochondrial membranes during which it is acted upon by enzymes including carnitine transporter (OCTN2), carnitine palmitoyltransferase-1 (CPT1), carnitine palmitoyltransferase-2 (CPT2), and carnitine acylcarnitine translocase (CACT) (Fig. 1) [1, 2]. Carnitine penetrates into cells across the plasma membrane against a high concentration gradient of free carnitine with the aid of the plasma membrane OCTN2 protein encoded by the SLC22A5 gene [3]. Deficiency of OCTN2 causes primary carnitine deficiency (PCD, OMIM 212140), which is characterized by systemic carnitine deficiency in tissues and blood but in concord with increased excretion of free L-carnitine in the urine [4–6]. Clinical symptoms in patients with PCD such as cardiomyopathy,

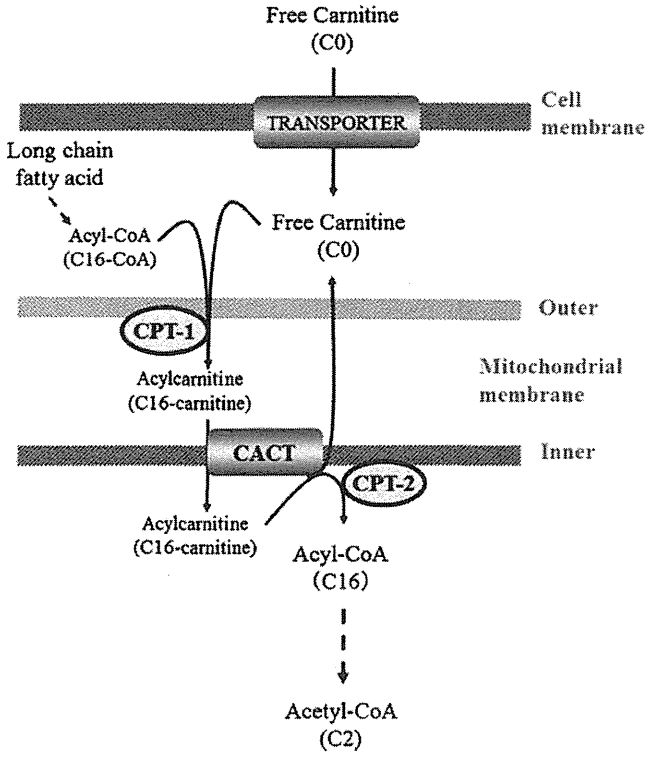

Fig. 1 Pathway for mitochondrial fatty acid beta-oxidation. Transporter: carnitine uptake transporter; *CPT-1*: carnitine palmitoyltransferase-1, *CACT*: carnitine acylcarnitine translocase, *CPT-2*: carnitine palmitoyltransferase-2. *Solid arrows* indicate single reactions; *dashed arrows* indicate multiple reactions or steps

encephalopathy, hepatomegaly, myopathy, hypoglycemia, and hyperammonemia, mainly result from low carnitine concentration in the tissues. On the other hand, secondary carnitine deficiency occurs in some conditions such as organic acidemias, renal dialysis, long-term medication (antiepileptic drugs or some antibiotics), and alimentary deficiency of L-carnitine [7–9].

It is necessary to make a differential diagnosis of PCD from the secondary carnitine deficiency or other false-positive cases, and diagnosis is confirmed by demonstrating reduced transport in skin fibroblasts from the patients. Until now, cluster-tray method using radioisotope-labeled substrate was used for the diagnosis of PCD [4, 10–12]. However, such a diagnostic method requires handling of radioactive substrates and focused only on diagnosis of PCD. Gene sequencing in SLC22A5 is one diagnostic method for PCD. However, it is molecularly heterogenous, and around 50 different mutations have been identified [6]. After acylcarnitine analysis using tandem MS analysis became available in the worldwide, blood acylcarnitine analysis was used as an initial method for diagnosis of FAO disorders and a detection of FAO disorders has been increased. However, it is necessary to confirm the diagnosis of the diseases with detailed analysis. The in vitro probe acylcarnitine (IVP) assay using cultured fibroblasts and tandem mass spectrometry (MS/MS) has been used to evaluate FAO capacity in the cultured cells and make a diagnosis of FAO disorders [13–15]. However, conventional IVP assay is not feasible to diagnose PCD or CPT1 deficiency, because excess amount of free carnitine is added to the experimental medium at the beginning. Estimation of free carnitine, which is the key marker for the above diseases, in experimental medium was nonsense for diagnosis of these disorders. We developed a novel functional assay for PCD and CPT1 deficiency using the IVP assay, with some modifications. This method uses different concentrations of exogenous free carnitine and measures intracellular as well as extracellular acylcarnitine (AC) levels, which overcomes the disadvantage of the conventional IVP assay in the diagnosis of carnitine cycle disorders.

Materials and methods

Materials

Hexanoylcarnitine (C6), octanoylcarnitine (C8), decanoylcarnitine (C10), and palmitoylcarnitine (C16) were purchased from Sigma–Aldrich (St Louis, MO, USA). Methanol, acetonitrile, and formic acid were purchased from Wako (Osaka, Japan). As an internal standard, a labeled carnitine standard kit (NSK-B), which contains $^{2}[H]_{9}$-carnitine, $^{2}[H]_{3}$-acetylcarnitine, $^{2}[H]_{3}$-propionylcarnitine, $^{2}[H]_{3}$-butyrylcarnitine, $^{2}[H]_{9}$-isovalerylcarnitine, $^{2}[H]_{3}$-octanoylcarnitine, $^{2}[H]_{9}$-myristoylcarnitine, and $^{2}[H]_{3}$-palmitoylcarnitine, was purchased from Cambridge Isotope Laboratories (Andover, MA, USA).

Preparation of standard solutions of ACs

Standard solutions containing 1, 10, 25, and 50 μmol/L each of C6, C8, C10, and C16 were used to validate the recovery and determine linear concentration range of ACs after extraction by the Folch method [16]. The ACs were dissolved in methanol (99.8 %), and the prepared standard solution was analyzed directly and after extraction by the Folch method.

Subjects

Human skin fibroblasts from six healthy controls (volunteers) and seven patients with various carnitine cycle disorders—three each with PCD and CPT2 deficiency and one with CPT1 deficiency—were analyzed. In all cases, diagnoses were confirmed by mass spectrometric analyses (gas chromatography-mass spectrometry and MS/MS), enzyme assay, and protein or mutational analyses. Informed consent was obtained from the patients or their families. This study was approved by the Ethical Committee of the Shimane University School of Medicine.

In vitro probe acylcarnitine (IVP) assay using MS/MS

An IVP assay was performed, as described, with some modifications [13, 15, 17], and principle of IVP assay was shown Fig. 2. Briefly, 3×10^6 cells were seeded in triplicate onto a six-well microplate (35 mm i.d.; Iwaki) and cultured until confluent. After washing twice with Dulbecco's phosphate buffered saline (DPBS; Invitrogen, Carlsbad, CA, USA), the cells were subsequently cultured for 96 h in 1 ml of a special experimental minimal essential medium (MEM) containing bovine serum albumin (0.4 % essential fatty acid-free BSA; Sigma), two different concentrations of C0 (Sigma)—10 μmol/L (reduced level, lower compared with physiological level) and 400 μmol/L (excess level)—and unlabelled palmitic acid (0.2 mmol/L; Nacalai Tesque). C0 and AC levels in the culture medium (extracellular fraction) and in the intracellular extract were analyzed after a 96-h incubation period using MS/MS (API 3000; Applied Biosystems, Foster City, CA, USA), as described [18].

Intracellular acylcarnitine extraction

Intracellular C0 and ACs were extracted using the Folch method, with some modification [16]. Briefly, harvested cells were washed twice with DPBS buffer. The cell pellet was resuspended in 100 μl volume of DPBS buffer and immediately frozen in liquid N_2. In order to separate phospholipids and cell debris, 250 μl of Folch reagent (chloroform/methanol, 2:1) was added to the resuspended cell pellet. After vigorous mixing using a vortex mixer, the solution was centrifuged for 10 min at 15,000 rpm at 4 °C. The debris layer around the interface between the aqueous and lipid phases was removed, and the extracted aqueous and lipid phases were mixed and thereafter dried under a nitrogen stream at 50 °C. ACs in culture medium supernatants and extracted intracellular ACs lysate were analyzed using MS/MS (API 3000; Applied Biosystems, Foster City, CA, USA). Briefly, methanol (200 μl) including an isotopically labeled internal standard (Cambridge Isotope Laboratories, Kit NSK-A/B, Cambridge, UK) was added to 10 μL of supernatant from culture medium and extracted intracellular ACs, for 30 min. Portions were centrifuged at 1,000×*g* for 10 min, and then 150 μL of supernatant was dried under a nitrogen stream and butylated with 50 μL of 3 N *n*-butanol-HCl at 65 °C for 15 min. The dried butylated sample was dissolved in 100 μL of 80 % acetonitrile/water (4:1 *v/v*), and then the ACs in 10 μL of the aliquots were determined using MS/MS [18] and quantified using ChemoView™ software (Applied Biosystems/MDS SCIEX, Toronto, Canada).

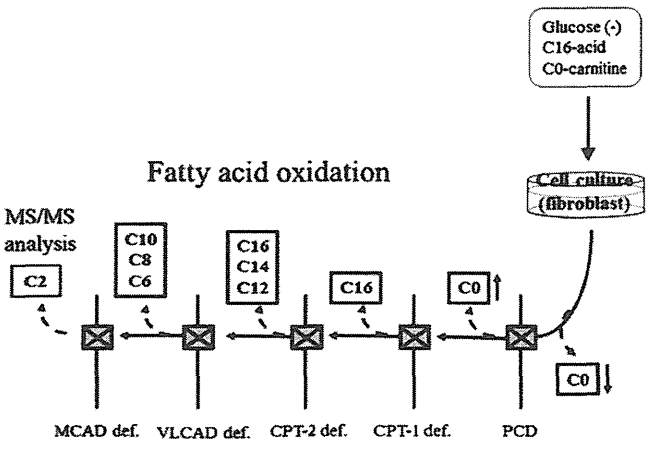

Fig. 2 Principle of in vitro probe acylcarnitine assay. *C2, C4, C6, C8, C10, C12, C14*, and *C16* represent acylcarnitines

Protein concentration and cell viability

Protein concentrations were measured by a modification of the Bradford method using the Bio-Rad protein assay (Bio-Rad, Hercules, CA, USA) [19]. The percentage of viable cells was determined at 24, 48, 72, and 96 h of incubation using the modified 3-(4,5-dimethyl-2-yl)-2, 5-diphenyl-2H-tetrazolium bromide (MTT) assay [20].

Data and statistical analysis

The results are expressed as mean±SD from at least three independent experiments for IVP assay in each cultured cell and three intra-assays and three inter-assays for recovery of standard AC solutions, and statistical significance was evaluated using Student's *t*test in Microsoft Excel. The AC concentrations were expressed as nanomoles per milligram protein.

Results

Recovery of ACs during Folch extraction

The AC standards in the aqueous or lipid fraction were analyzed separately using MS/MS, after extraction by the Folch procedure, and compared with direct analysis of the total mixed standard solutions using three inter-assays and three intra-assays of analysis of standard AC solution. As shown in Fig. 3, most of the C6 and C8-carnitines fractionated to the aqueous phase, while almost all C16-carnitine was exclusively retained in the lipid phase. The amount of C10-carnitine was comparable in both aqueous and lipid phases.

To determine the loss of C0 and ACs during Folch extraction, the standard AC solution was analyzed directly after routine sample preparation for MS/MS and compared with that after Folch extraction. The recovery of ACs in the